NEUROSCIENCE

A neural circuit linking two sugar sensors regulates satiety-dependent fructose drive in *Drosophila*

Pierre-Yves Musso, Pierre Junca, Michael D. Gordon*

In flies, neuronal sensors detect prandial changes in circulating fructose levels and either sustain or terminate feeding, depending on internal state. Here, we describe a three-part neural circuit that imparts satiety-dependent modulation of fructose sensing. We show that dorsal fan-shaped body neurons display oscillatory calcium activity when hemolymph glucose is high and that these oscillations require glutamatergic input from SLP-AB or "Janus" neurons projecting from the protocerebrum to the asymmetric body. Suppression of activity in this circuit, either by starvation or by genetic silencing, promotes specific drive for fructose ingestion. This is achieved through neuropeptidergic signaling by tachykinin, which is released from the fan-shaped body when glycemia is high. Tachykinin, in turn, signals to Gr43a-positive fructose sensors to modulate their response to fructose. Together, our results demonstrate how a three-layer neural circuit links the detection of two sugars to produce precise satiety-dependent control of feeding behavior.

INTRODUCTION

Sugars represent an important energy source for many animals, including humans and fruit flies. Although the three most common dietary sugars—glucose, fructose, and sucrose—all have the same caloric value, they differ in both their sensory and metabolic properties. Glucose supports the energetic needs of tissues throughout the body, and mammalian blood glucose (glycemia) is under tight hormonal control, with insulin triggering glucose uptake by cells upon feeding and glucagon triggering glycogenolysis upon starvation. Glucose absorbed by the gut after a meal can produce moderate glycemic elevation that triggers satiety responses including repression of the orexigenic hormone ghrelin, stimulation of anorexigenic leptin, and suppression of the hypothalamic energy sensor adenosine 5′-monophosphate–dependent protein kinase (AMPK). By contrast, fructose, which is a favored additive in modern processed foods because of its intense sweetness, must be metabolized to glucose before energy utilization. Mammalian blood fructose levels remain low but can rise >50-fold after a sugary meal (*1*, *2*). Moreover, fructose can actually elevate AMPK activity and drive further feeding through the stimulation of agouti-related peptide (AgRP) neurons and suppression of pro-opiomelanocortin neurons of the hypothalamus (*3*). Thus, a robust system to ensure appropriate carbohydrate intake would likely need to integrate the differential properties of these important sugars.

Lowered glycemia is an important trigger for hunger and food seeking in mammals and *Drosophila* (*4*, *5*). In flies, glucose and trehalose circulate in the hemolymph, and the concentration of each is reduced upon starvation (*6*). Several neurons have been suggested to directly sense glucose and affect feeding behavior, including neurons expressing the peptide DH44, a homolog of the mammalian corticotropin-releasing hormone (*7*), and "*CN* neurons," which coexpress the GnRH homolog corazonin (Crz) and the neuropeptide Y (NPY) homolog short neuropeptide F (sNPF) (*8*, *9*). Both populations display oscillatory calcium activity in the presence of circulating nutritive sugars and are necessary for postingestive nutrient selection (*7*, *9*). MB-MP1 neurons of the mushroom bodies (MBs) also display calcium oscillations at a frequency around 0.1 Hz and are thought to signal the availability of energy required for long-term memory (LTM) formation (*10*, *11*). This 0.1-Hz frequency is notably slow compared to other characterized oscillations involved in visual and olfactory perception (*12*, *13*), motor coordination (*14*), memory (*15*, *16*), and sleep and consciousness (*17*, *18*). The slow frequency of energy sensing oscillations in flies may be a criterion for identifying functionally similar neurons.

In addition to the role of glucose in satiety, sugars are known to evoke appetitive postingestive responses. Gastric infusion of sugars can drive positive flavor associations, and sucrose consumption elicits taste-independent preference and striatal dopamine release in sweet-blind mice (*19*, *20*). Similarly, flies show taste-independent preference for feeding on nutritional sugars and require postingestive energy sensing to form long-term memories (*5*, *7*, *10*, *11*, *21*–*23*). Although several neurons have been posited to mediate postingestive sugar sensing in flies, one population of particular interest is in the lateral protocerebrum and expresses the gustatory receptor (GR) family member Gr43a. Gr43a is one of nine identified sugar-sensing GRs, all of which are expressed in subsets of peripheral gustatory receptor neurons (GRNs) housed in taste organs of the proboscis and legs (*24*–*26*). However, Gr43a is unusual in that it is also expressed in the central brain, and it is specifically tuned to fructose. When flies consume a sugary meal, total internal fructose levels rise markedly and activate the so-called "Gr43a brain neurons." The activity of Gr43a brain neurons then drives feeding prolongment in hungry flies and feeding cessation in those that are sated (*24*).

One appealing aspect of specifically sensing postingestive fructose is that it cleanly separates detection of ingested sugars from glucose-driven changes in satiety. Naturally occurring sweet foods generally contain both fructose and glucose, as well as sucrose, which is a dimer of the two. Thus, internal fructose may serve as the cue for recently ingested sugar and vary widely, while tightly controlled glucose levels provide a satiety signal that modulates fructose sensing and other state-dependent behaviors. Although available behavioral and physiological data support this model, the circuitry connecting starvation and glycemia with fructose sensing by Gr43a brain neurons has not been explored.

Department of Zoology and Life Sciences Institute, University of British Columbia, Vancouver, Canada.
*Corresponding author. Email: gordon@zoology.ubc.ca

In this study, we find that neurons in dorsal layers of the central complex structure called the fan-shaped body (FB) act as central glucose sensors that couple satiety state with fructose drive. These dorsal FB (dFB) neurons display calcium oscillations in fed flies, which have equal preference between feeding on fructose or glucose. However, prolonged starvation suppresses dFB oscillations and leads to a strong shift in preference toward fructose. We show that silencing dFB neurons mimics the fructose preference shift seen upon prolonged starvation and that dFB activity is modulated by glutamatergic inputs from the superior lateral protocerebrum. Last, we demonstrate that the effect of dFB neurons on fructose feeding is mediated by release of the neuropeptide tachykinin, which signals to Gr43a brain neurons. The linking of two specific sugar sensors in this three-neuron circuit imparts precise hunger-dependent control over sugar consumption.

RESULTS

Starvation regulates FB oscillations

To identify previously unknown circuits controlling carbohydrate intake, we surveyed calcium activity in candidate brain areas using GCaMP6f expression under control of GAL4 lines from the Janelia Flylight collection (*27*, *28*). This revealed oscillatory activity in dFB neurons labeled by *R70H05-GAL4* (Fig. 1A and table S1). We noted asymmetry in the oscillations, with asynchronous activity on the right and left side, and a tendency for the right part of the dFB to show higher frequencies than the left, although this difference is not statistically significant (fig. S1, A and B, and movie S1). Oscillations were strong in fed flies and progressively reduced in intensity and frequency after increasing starvation times up to 30 hours (Fig. 1, B to F; fig. S1, A and B; and movies S1 and S2). Because starvation is associated with lower hemolymph carbohydrate levels (*5*), we hypothesized that dFB neurons may act as brain glucose sensors. Knocking down glucose transporter type 1 (Glut1) and hexokinase C (HexC) within dFB reduced their oscillations to a level comparable to prolonged starvation. This supports a role for glucose sensing in dFB regulation, although we cannot rule out contributions of indirect mechanisms coupling dFB activity with other glucose-sensitive populations (Fig. 1, B to F, and fig. S1, A and B) (*5*, *9*, *29*, *30*).

AB-FBl8 (dFB) neurons drive starvation-dependent changes in fructose feeding

The dFB neurons labeled by *R70H05-GAL4* occupy layers 8 and 9 of the FB and project to the asymmetric body (AB), identifying them as AB-FBl8 (or vΔA_a) neurons (Fig. 2A) (*28*, *31*–*33*). For simplicity, we will refer to them simply as dFB. To test whether dFB neurons link satiety signals to changes in behavior, we silenced them and measured feeding using a modified version of flyPAD, where food interactions were calculated using the algorithm we developed for the sip-triggered optogenetic behavior enclosure (STROBE) (Fig. 2, B and C) (*34*, *35*). Flies conditionally expressing the inward rectifying potassium channel Kir2.1 under the control of *R70H05-GAL4* and *tub-Gal80^{TS}* displayed an increased number of interactions with sucrose at low concentrations (5 and 50 mM) but not at 1 M (Fig. 2D). dFB silencing did not affect feeding on either L-glucose (sweet but not caloric) or sorbitol (caloric but not sweet) but markedly elevated interactions with a mixture of the two (Fig. 2, E to G) (*10*). Given that the sweet taste of sucrose and L-glucose stimulates feeding initiation, we suspected that sorbitol and sucrose were being detected

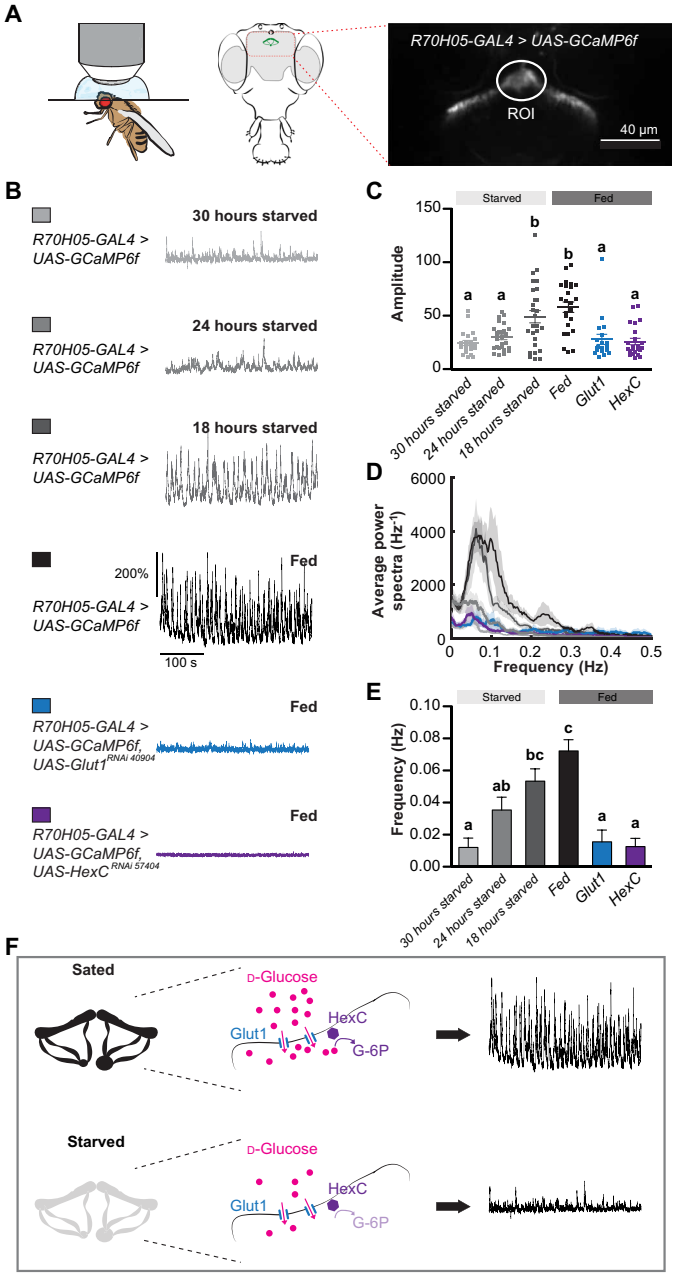

Fig. 1. Starvation regulates FB oscillations. (**A**) Schematic of imaging preparation to monitor calcium oscillations (left) with GCaMP6f signal from *R70H05-GAL4* expression in the dFB (right). (**B**) Calcium traces from *R70H05-GAL4* > *UAS-GCamP6f* flies after different periods of starvation or expressing RNAi against Glut1 or HexC. (**C**) Amplitudes of dFB oscillations. (**D**) Power spectra of dFB oscillations. (**E**) Frequencies of dFB oscillations. (**F**) Model: In sated flies, D-glucose enters the dFB neurons through Glut1 and triggers oscillations through the activity of HexC; in starved flies, the low availability of D-glucose prevents oscillations. Values represent mean ± SEM. $n = 19$ to 27. Statistical tests: one-way analysis of variance (ANOVA) and Tukey post hoc; different letters represent significant differences $P < 0.05$.

postingestively to trigger enhanced feeding in dFB-silenced flies. D-Glucose failed to trigger excess feeding by dFB-silenced flies, indicating that energy alone was not sufficient for this postingestive effect (Fig. 2H). However, fructose, which is quickly metabolized

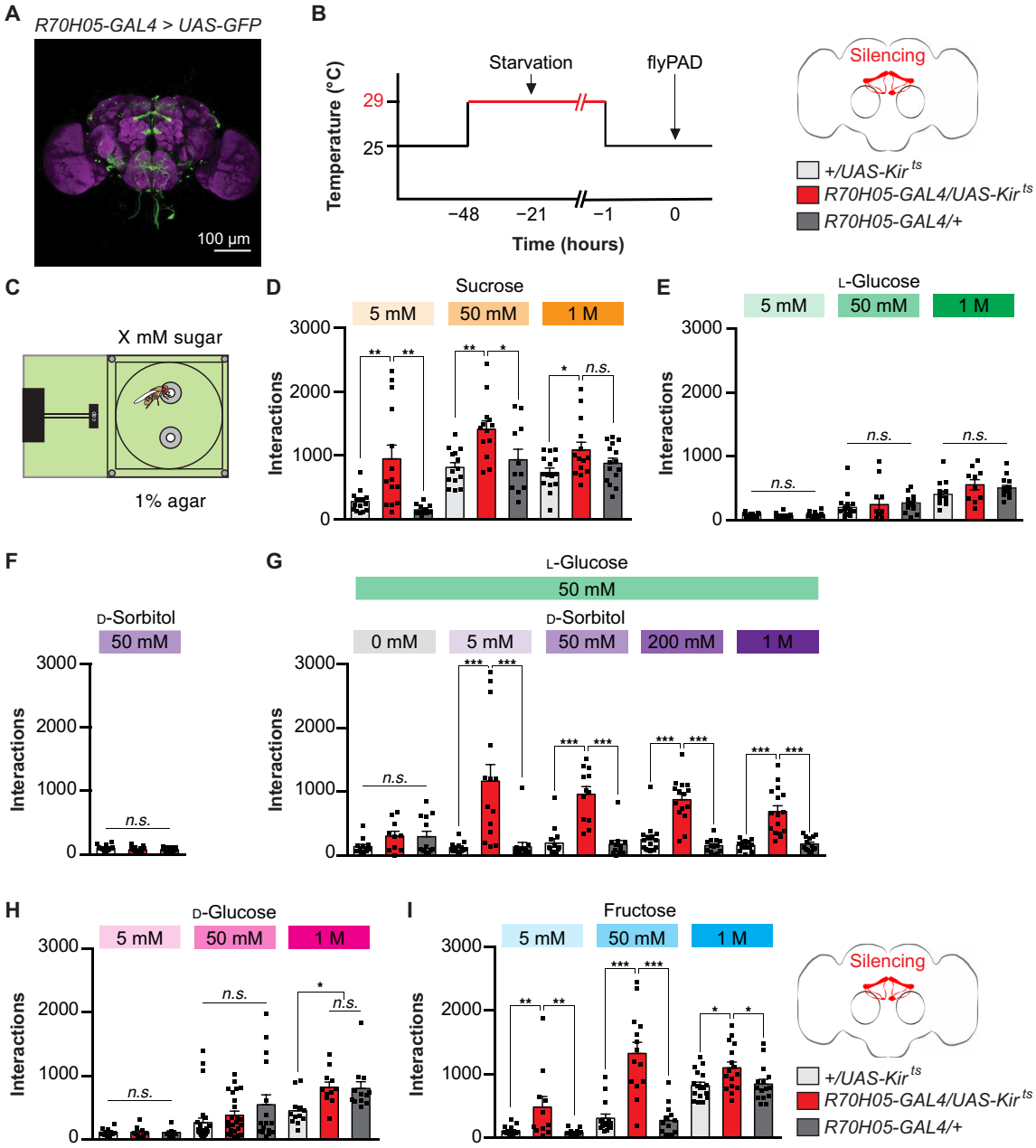

Fig. 2. Silencing dFB neurons increases fructose feeding. (**A**) Immunofluorescent detection of *UAS-GFP* driven by *R70H05-GAL4*. (**B**) Experimental timeline: Flies are placed at 29°C for 47 hours and starved for 18 hours, and experiments are performed at 25°C . (**C**) Experimental setup: One channel is filled with sugar and the other one is filled with 1% agar. (**D**) Effect of dFB neuron silencing on interactions with various concentrations of sucrose (5, 50, and 1000 mM; $n = 16$ to 21). *UAS-Kir*^{ts} represents *UAS-Kir2.1* plus *tub-Gal80*^{ts}. (**E**) Effect of dFB neuron silencing on interactions with various concentrations of L-glucose (5, 50, and 1000 mM; $n = 10$ to 19). (**F**) Effect of dFB neuron silencing on interactions with 50 mM D-sorbitol ($n = 15$). (**G**) Effect of dFB neuron silencing on interactions with 50 mM L-glucose mixed with various concentrations of D-sorbitol (0, 5, 50, 200, and 1000 mM; $n = 10$ to 16). (**H**) Effect of dFB neuron silencing on interactions with various concentrations of D-glucose (5, 50, and 1000 mM; $n = 8$ to 26). (**I**) Effect of dFB neuron silencing on flies' interactions with various concentrations of fructose (5, 50, and 1000 mM; $n = 11$ to 17). Values represent mean ± SEM. Statistical tests: one-way ANOVA and Tukey post hoc; ns, $P > 0.05$; *$P < 0.05$; **$P < 0.01$; ***$P < 0.001$.

from both sucrose and sorbitol (*24*), elicited strongly enhanced feeding in dFB-silenced flies (Fig. 2I). Thus, we posited that dFB is part of a circuit that links satiety-dependent changes in hemolymph glucose levels with a fly's response to postingestive changes in internal fructose.

If dFB produces satiety signals that inhibit postingestive fructose sensing, then suppressing dFB activity should release this inhibition and produce increased relative preference for fructose over glucose. We found that flies with silenced *R70H05-GAL4* neurons displayed a strong preference for fructose over glucose at concentrations of

5 and 50 mM, but not 1 M, while control flies showed nearly equal preference for the two sugars at all concentrations (Fig. 3, A and B, and fig. S1C). Because *R70H05-GAL4* drives expression in additional neurons outside the dFB, we verified the causal role for dFB by measuring glucose versus fructose preference after silencing with two other drivers (*R70H05-LexA* and *VT005528-GAL4*) and a split construction that we built (*dFB-split*), all of which specifically label dFB neurons (fig. S1, D to F). In each case, dFB silencing led to a strong preference for fructose over glucose. This effect holds true for mated females (the original test subjects), males, and virgin females (fig. S1, F to H). We also verified that dFB neurons labeled by *dFB-split* showed oscillatory activity that was reduced after prolonged starvation (fig. S1, I to K).

Given that dFB oscillations are suppressed upon starvation, we wondered whether dFB silencing evoked a starvation-like state in flies. We subjected dFB-silenced and control flies to different periods of food deprivation and then measured their preference for fructose versus glucose (Fig. 3C). Both dFB-silenced and control flies preferred fructose over glucose after food deprivation of 24 hours or more, while only the dFB-silenced flies preferred fructose after 16 hours without food (Fig. 3D). The timing of wild-type flies' shift in preference toward fructose correlates well with their reduction in dFB calcium oscillations, which are significantly suppressed after 24 hours of starvation (Fig. 1B). Moreover, refeeding flies with glucose after 30 hours of starvation restored oscillations, while equivalent refeeding with fructose did not (Fig. 3E). Thus, glucose, but not fructose, "reactivates" the dFB, allowing separation of dFB regulation by glucose from dFB's effects on fructose drive.

Notably, preference between fructose and glucose was equal for all groups after 0 or 8 hours of starvation. We suspect that this is because a threshold of consumption needs to be met for postingestive fructose sensing to stimulate further feeding and that feeding initiation is controlled independently of dFB activity. Thus, flies without sufficient food deprivation do not consume enough fructose to trigger dFB-regulated feeding circuits. To test this idea, we measured the proboscis extension reflex (PER), where the probability of a fly extending its proboscis after brief stimulation of its taste neurons produces a quantitative readout of taste appetitiveness (*26*, *36*, *37*). The PER to fructose and glucose remained unchanged after dFB silencing in flies starved 21 hours, indicating that dFB neurons do not regulate peripheral sensitivity to sugars or sensory-driven feeding initiation, and likely rather modulate responses to postingestive cues (fig. S2, A and B).

Although food interactions measured on the flyPAD strongly correlate with consumption, we next sought to confirm that dFB silencing genuinely promotes fructose ingestion. As expected, dFB-silenced flies preferentially consumed fructose over glucose in a dye-based binary choice feeding assay, while controls consumed the two sugars equally (fig. S2C). Moreover, control flies preferentially consumed fructose over glucose when dFB activity was reduced by 43 hours of starvation, and thermogenetic activation of dFB with transient receptor potential A1 (TRPA1) suppressed this elevated fructose feeding (fig. S2D). This demonstrates that dFB activity is sufficient to inhibit fructose sensing mechanisms in starved flies.

To link the behavioral role of dFB back to their function in glucose sensing, we measured the feeding preference of flies after RNAi knockdown of Glut1 or HexC in the dFB. Consistent with their effects on dFB oscillations, knockdown of either gene promoted strong preference for fructose over glucose in the flyPAD (Fig. 3, F and G, and fig. S3, A and B). This suggests that changes in dFB activity mediated by glucose sensing drive effects on fructose feeding. Together, our results indicate that starvation-induced reduction of hemolymph glucose suppresses dFB activity, which, in turn, promotes fructose feeding (Fig. 3H).

Janus neurons synaptically modulate dFB oscillations

To examine the broader circuit in which dFB are regulating fructose consumption, we used *UAS-synaptotagmin-GFP* (*UAS-Syt-GFP*) and *UAS-DenMark* to label pre- and postsynaptic areas, respectively. This demonstrated that the dFB presynaptic terminals reside in layers 8 and 9 of the FB, while their dendrites primarily occupy the AB, a structure known to be required for energy-intensive LTM (Fig. 4A) (*10*, *21*, *23*, *38*). In search of inputs to dFB, we examined the superior lateral protocerebrum (SLP)–AB population, which has arborizations in the SLP and the AB (*28*, *32*). On the basis of the shape and slight asymmetry in the bilateral mirror image of these neurons, we decided to call them "Janus neurons" in reference to the two-faced representation of the Roman god. We generated a split-GAL4 labeling Janus neurons and confirmed the location of their dendrites in the SLP and axon terminals in the AB (Fig. 4B). Trans-Tango driven by this driver revealed postsynaptic neurons in layers 8 and 9 of the FB, suggesting that dFB are postsynaptic to Janus neurons (Fig. 4C) (*39*). Moreover, green fluorescent protein (GFP) reconstitution across synaptic partners (GRASP) between dFB and Janus revealed a single point of contact in the AB (Fig. 4D). Last, Janus neurons do not display spontaneous calcium activity but silencing them reduced the oscillatory activity of dFB in fed flies, demonstrating functional connectivity between the two neuron populations (Fig. 4, E to H, and fig. S3C).

Next, we addressed whether the modulatory action of Janus neurons on dFB affects behavior. Silencing Janus neurons reproduced all the behavioral phenotypes observed from dFB silencing: increased feeding interactions with sucrose, fructose, and a mixture of L-glucose and sorbitol, but not D-glucose, L-glucose, or sorbitol alone (fig. S4, A to H); no effect on taste sensitivity to fructose or D-glucose (fig. S4, I and J); and enhanced preference for fructose over glucose (Fig. 5A and fig. S4K). Silencing Janus with an independent driver [*R72A10-LexA* (*28*)] also reproduced the fructose feeding preference, verifying that Janus was responsible for this phenotype (fig. S5L). Moreover, like dFB, Janus thermogenetic activation with TRPA1 reduced fructose feeding preference in strongly starved flies (fig. S4M).

Knocking down Glut1 and HexC in Janus neurons did not affect behavior, suggesting that these neurons do not sense hemolymph D-glucose (fig. S5, A and B). Further, this serves as a control demonstrating that the impaired oscillations observed in dFB neurons after the same treatment is due to a specific function in glucose sensing rather than a nonspecific effect on cell viability. Knockdown of the vesicular glutamate transporter (Vglut) in Janus neurons promoted fructose feeding preference, suggesting that Janus neurons exert their effect on dFB via glutamate (Fig. 5B and fig. S5, C to E). We performed an RNA interference (RNAi) screen targeting the different glutamate receptors in the dFB and found that knocking down GluClα, KaiR1D, NmdaR1, and NmdaR2 also induced fructose preference and decreased dFB oscillations (Fig. 5, C to E, and fig. S5, F to M) (*40*–*42*). Together, these data suggest that Janus neurons affect behavior by promoting dFB oscillations via the action of glutamate on multiple receptors (Fig. 5E).

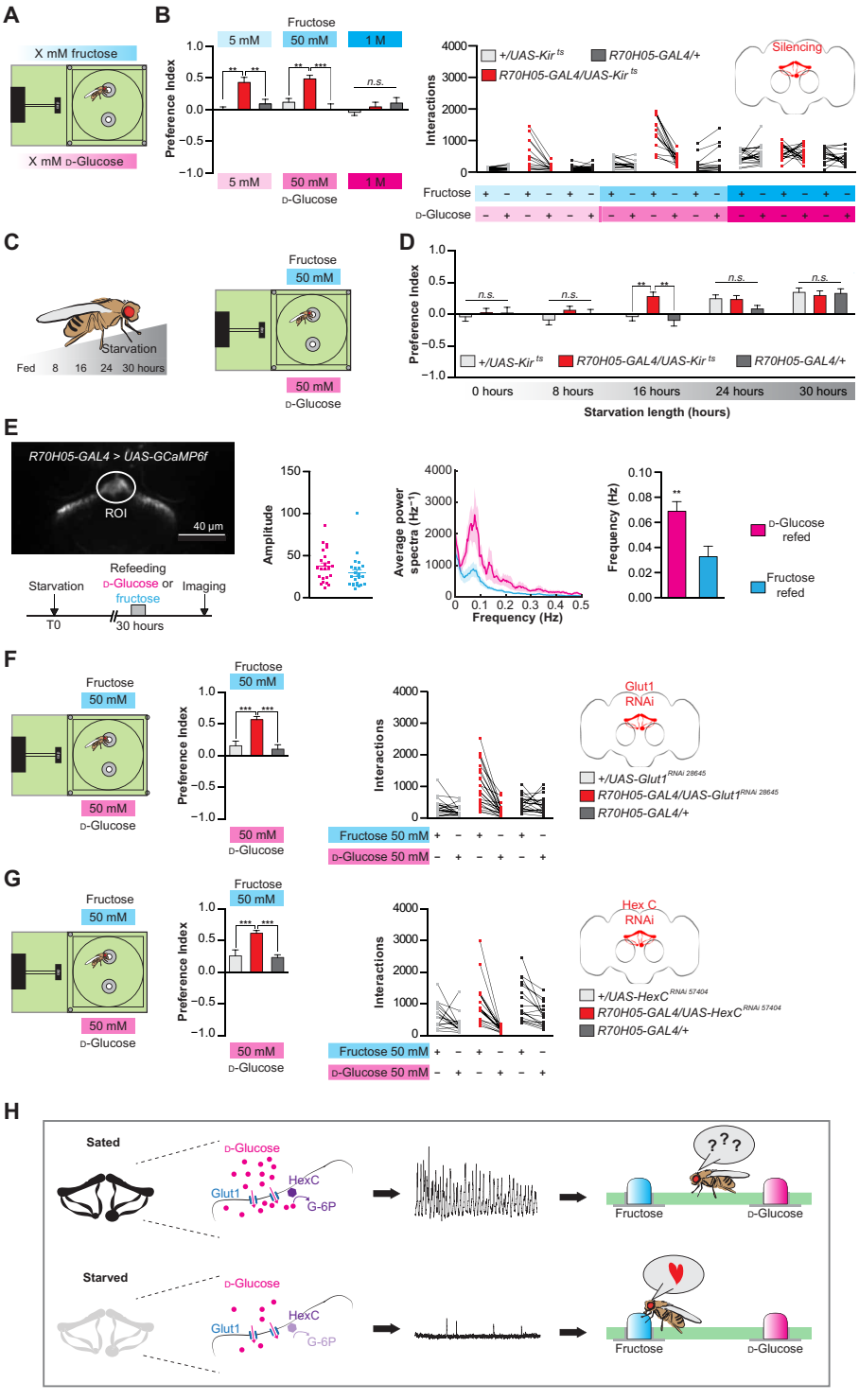

Fig. 3. Fructose feeding preference relies on starvation. (**A**) Experimental setup: The left channel is filled with fructose and the right channel is filled with the same concentration of D-glucose. (**B**) Effect of dFB neuron silencing on flies' preference between fructose and D-glucose at different concentrations after 20-hour starvation (left) and their corresponding interactions (right; $n = 13$ to 21). (**C**) Experimental setup: Flies are starved for different amounts of time and given the choice between 50 mM fructose and 50 mM D-glucose. (**D**) Effect of starvation length on preference between 50 mM fructose and 50 mM D-glucose in controls and flies with silenced dFB neurons ($n = 21$ to 36). (**E**) Refeeding 30-hour starved flies with 500 mM D-glucose for 30 min restores oscillations in dFB, while 500 mM fructose does not ($n = 23$). (**F**) Effect of knocking down Glut1 in dFB neurons on the preference between 50 mM fructose and D-glucose after 20-hour starvation ($n = 19$ to 23). (**G**) Effect of HexC knockdown in dFB neurons on preference between 50 mM fructose and D-glucose after 20-hour starvation ($n = 15$ to 18). (**H**) Model for regulation of fructose preference by dFB activity. Values represent mean ± SEM. Statistical tests: one-way ANOVA and Tukey post hoc; ns, $P > 0.05$; $^{**}P < 0.01$; $^{***}P < 0.001$.

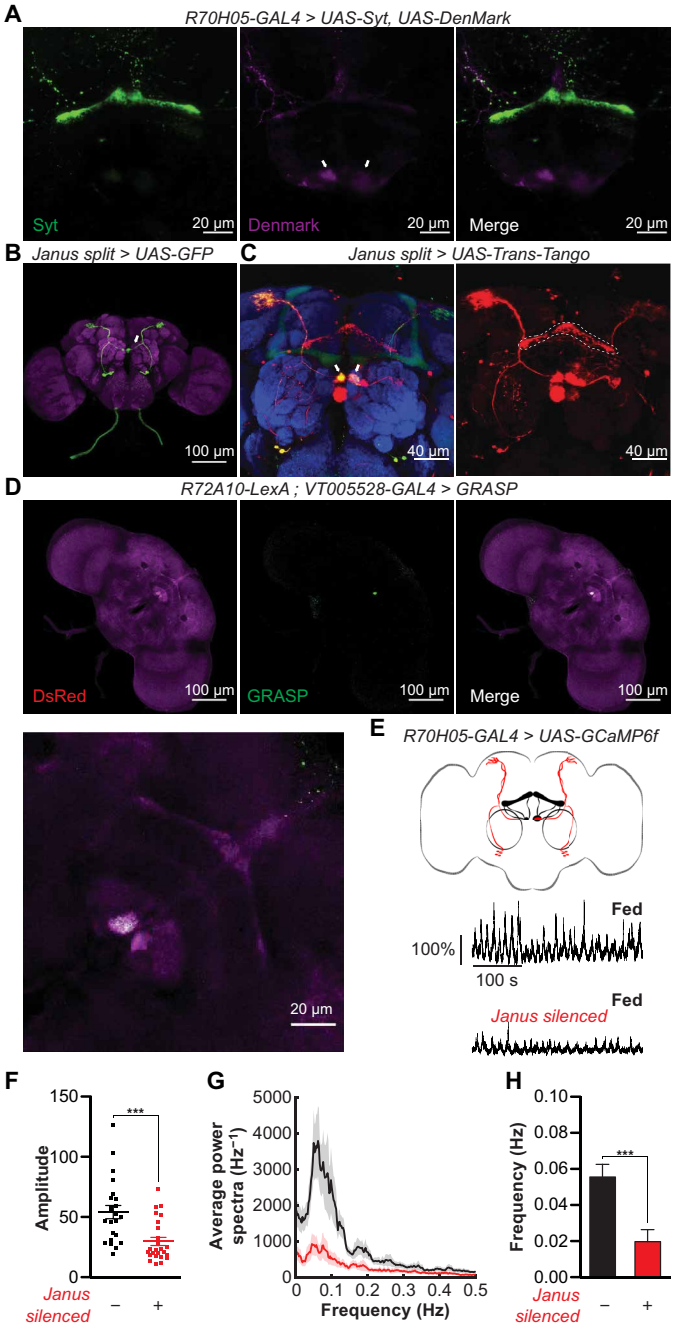

Fig. 4. Janus neurons contact dFB neurons on the asymmetric body and modulate oscillations. (**A**) Immunofluorescent detection of *UAS-Syt* (green) and *UAS-DenMark* (magenta) driven by *R70H05-GAL4*. Arrows show dendritic compartment localized on the asymmetric body. (**B**) Immunofluorescent detection of *UAS-GFP* driven by Janus split-GAL4. Arrows show projections to the asymmetric body. (**C**) Trans-Tango expression driven by Janus split-Gal4. Arrows show the contact between Janus neurons and postsynaptic targets, and the dotted line outlines *trans*-Tango expression in the FB layer 8. (**D**) GRASP between dFB and Janus neurons produces a signal at the asymmetric body. (**E**) Calcium trace from *R70H05-GAL4 > UAS-GCamP6f* (top) and *R70H05-GAL4; R72A10-LexA > UAS-GCamP6f; LexAop-tnt* (bottom) fed flies. (**F**) Amplitudes of oscillations. (**G**) Power spectra of oscillations. (**H**) Frequencies of oscillations. Imaging data are from ROI placed in the middle part of dFB neurons. Values represent mean ± SEM. $n = 23$ to 25. Statistical test: *t* test, ***$P < 0.001$.

dFB regulates fructose feeding via tachykinin signaling to Gr43a neurons

Initiating *trans*-Tango from the dFB did not show any clear postsynaptic targets, with the exception of the noduli (fig. S6, A and B). Such an absence of *trans*-tango signal suggests that dFB may function nonsynaptically through peptide secretion, which is characteristic of calcium oscillatory cells (*43*). This is supported by electron microscopy data revealing postsynaptic connections only within the FB and the AB and a previous report of tachykinin and sNPF expression in dFB (*41*, *44*–*47*). Moreover, immunostaining revealed stronger Tk expression in the dFB cell bodies of starved flies compared to fed flies, suggesting more Tk release in fed flies, where dFB oscillations are strong (Fig. 6, A and B). A recent study also showed elevated Tk mRNA expression in fed and re-fed flies compared to those that had been starved, indicating that starvation may regulate both Tk expression and release (*47*). Using two independent dFB drivers, we found that knockdown of Tk, but not sNPF, reproduced the fructose preference phenotype seen with dFB silencing (Fig. 6, C to E, and fig. S6, C and D).

Flies express two receptors for Tk: TkR86C [or neurokinin receptor (NKD)] (*48*–*50*) and the widely expressed TkR99D [or Drosophila tachykinin receptor (DTKR)] (*47*, *51*, *52*). Because Gr43a-expressing neurons in the lateral protocerebrum are the only known postingestive fructose sensors, we knocked down each receptor specifically in Gr43 brain neurons using *Gr43a-GAL4* combined with $Cha^{7.4kb}$*-GAL80* (fig S7, A and B) (*24*). This revealed a requirement for TkR99D, but not TkR86C, in restricting fructose intake (Fig. 7, A to C, and fig. S7, C and D). In vivo, TkR99D has been demonstrated to have inhibitory activity (*51*, *52*). Thus, we postulate that under fed conditions, Tk released from dFB inhibits brain Gr43a neurons, preventing them from responding to internal fructose, and thereby preventing feeding promotion by fructose ingestion (Fig. 7C).

Brain Gr43a neurons acutely regulate fructose feeding

To understand how Gr43a brain neurons affect feeding, we first tested their role in the choice between fructose and glucose using the flyPAD. Starved flies expressing Kir2.1 in Gr43a brain neurons under control of *Gr43a-GAL4* and $Cha^{7.4kb}$*-GAL80* strongly preferred glucose over fructose (Fig. 8A and fig. S8CA). Knocking down Gr43a in Gr43a brain neurons reproduced the same effect on preference but with a significantly lower number of interactions on fructose, confirming that these neurons require the Gr43a receptor for fructose detection (Fig. 8B). Because Gr43a brain neurons also express another "classic" sugar receptor called Gr64a, we also tested the function of this receptor (*26*). Unexpectedly, knocking down Gr64a in Gr43a brain neurons led to an increased preference for fructose, driven by increased interactions with the fructose option (Fig. 8C). Although Gr43a brain neurons express the short neuropeptide/hormone corazonin (*25*), knocking down corazonin in Gr43a brain neurons did not lead to any modification of the preference (fig S8B). Thus, Gr43a brain neurons likely exert their effect on fructose drive through a different pathway.

To test the sufficiency of Gr43a brain neurons to promote feeding, we used the STROBE to optogenetically activate Gr43a brain neurons in a closed-loop setup (Fig. 8D and fig. S8C). In this experiment, flies expressing the red light–activated channel CsChrimson in Gr43a brain neurons and previously fed the obligate CsChrimson cofactor all-trans retinal were compared to a control group without retinal (*53*). Flies could feed on either of two identical drops of 1% agar, one of which was coupled to red light activation. We found that the retinal-fed group robustly preferred the light-triggering

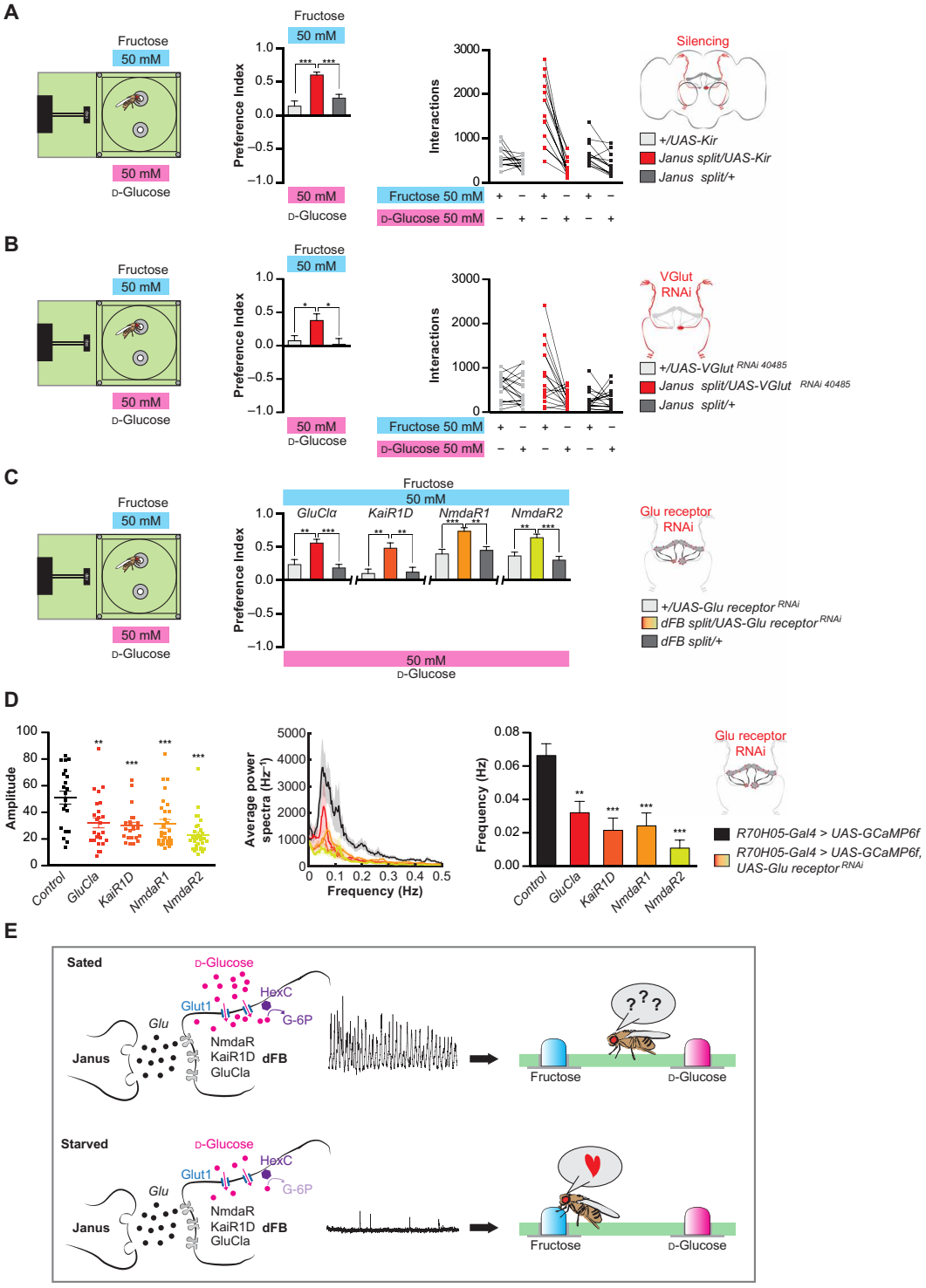

Fig. 5. Janus neurons act on dFB via glutamate acting on multiple receptors. (**A**) Effect of silencing Janus neurons on preference between fructose and D-glucose after 20-hour starvation and their corresponding interactions ($n = 13$ to 14). (**B**) Effect of *Vglut* knockdown in Janus neurons on preference between fructose and D-glucose after 20-hour starvation and their corresponding interactions ($n = 16$ to 19). (**C**) Effect of knocking down *GluClα*, *KaiR1D*, *NmdaR1*, and *NmdaR2* in dFB neurons on preference between fructose and D-glucose after 20-hour starvation and their corresponding interactions (for *GluClα*, $n = 14$ to 19; *KaiR1D*, $n = 25$ to 28; NmdaR1, $n = 18$ to 20; NmdaR2, $n = 23$ to 24). (**D**) Knocking down *GluClα*, *KaiR1D*, *NmdaR1*, and *NmdaR2* in dFB neurons moderately inhibits oscillations in fed flies (for controls, $n = 21$; *GluClα*, $n = 25$; *KaiR1D*, $n = 23$; NmdaR1, $n = 29$; NmdaR2, $n = 31$). (**E**) Glutamatergic input from Janus neurons is permissive for dFB oscillations. Values represent mean ± SEM. Statistical tests: one-way ANOVA and Tukey post hoc; ns, $P > 0.05$; *$P < 0.05$; **$P < 0.01$; ***$P < 0.001$.

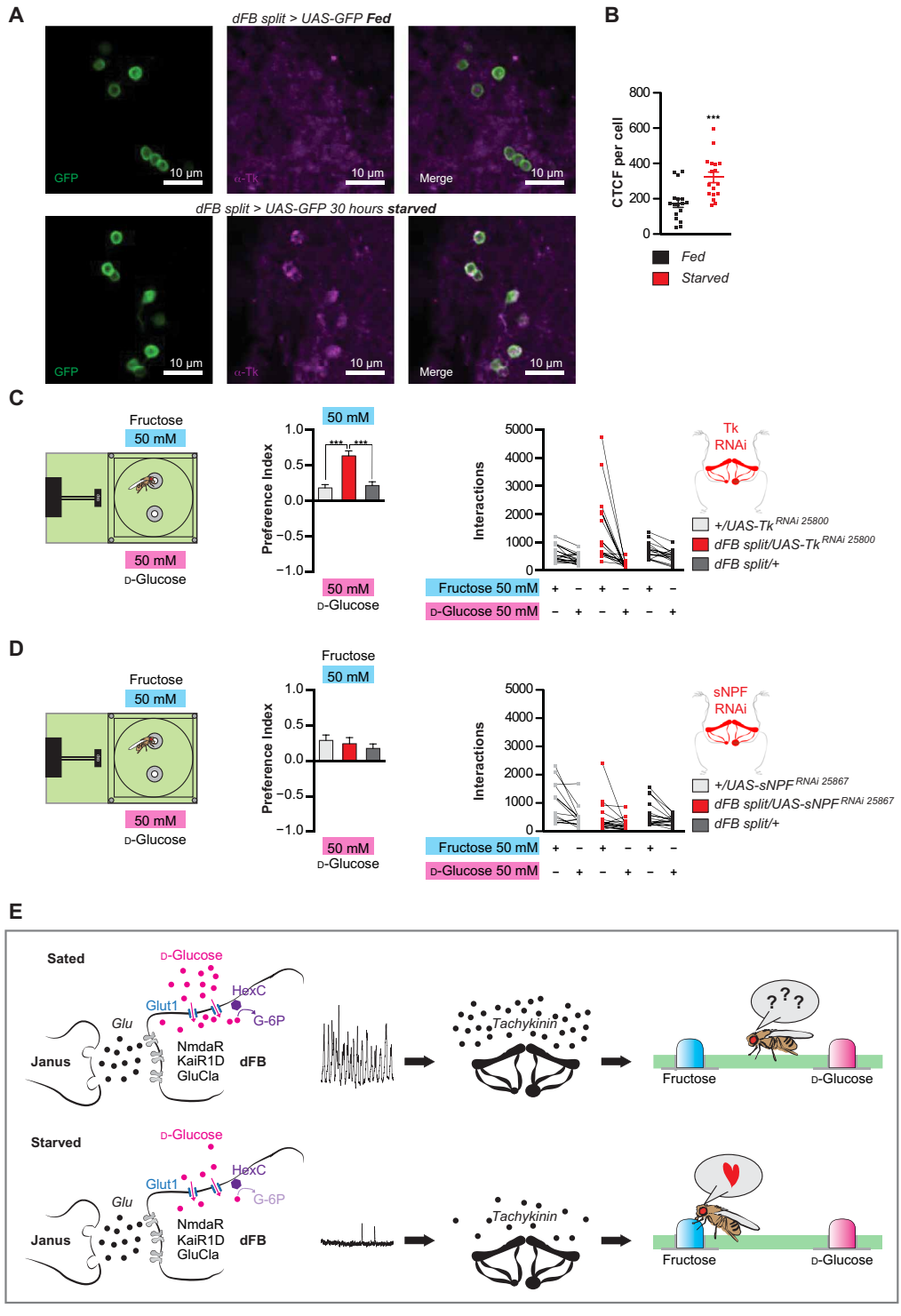

Fig. 6. dFB neurons regulate fructose-feeding preference through tachykinin release. (**A**) Immunofluorescent detection of *UAS-GFP* (green) driven by *dFB-split* and tachykinin (magenta) in the dFB cell bodies in fed flies (top) and flies starved for 30 hours (bottom). (**B**) Tachykinin peptide levels are lower in fed flies compared to flies starved for 30 hours ($n = 17$). CTCF, corrected total cell fluorescence. (**C**) Effect of knocking down tachykinin in dFB neurons on preference between fructose and D-glucose after 20-hour starvation and their corresponding interactions ($n = 16$ to 20). (**D**) Effect of sNPF knockdown in dFB neurons on preference between fructose and D-glucose after 20-hour starvation and their corresponding interactions ($n = 14$ to 18). (**E**) Tachykinin secretion in sated flies inhibits fructose feeding preference. Values represent mean ± SEM. Statistical tests: one-way ANOVA, Tukey post hoc for behavior, and *t* test for peptides levels. ns, $P > 0.05$; ***$P < 0.001$.

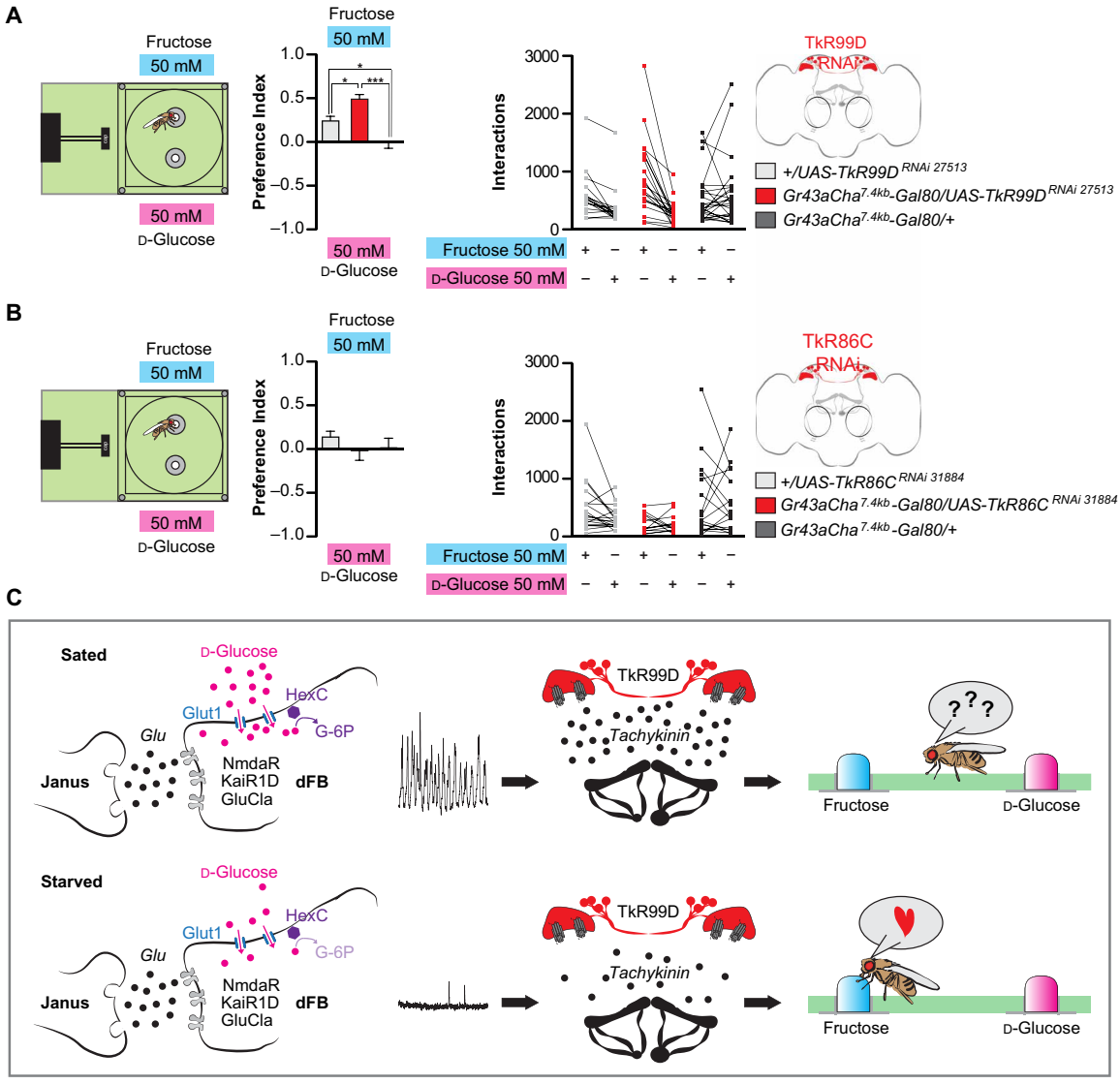

Fig. 7. Tachykinin acts through TkR99D to regulate Gr43a brain neurons and fructose-feeding preference. (**A**) Effect of TkR99D knockdown in Gr43a brain neurons on preference between fructose and D-glucose after 20-hour starvation and their corresponding interactions ($n = 18$ to 26). (**B**) Effect of TkR86C knockdown in Gr43a brain neurons on preference between fructose and D-glucose after 20-hour starvation and their corresponding interactions ($n = 14$ to 19). (**C**) Model: Tachykinin secretion in sated flies inhibits fructose feeding preference by acting on TkR99D expressed in Gr43a neurons. Values represent mean ± SEM. Statistical tests: one-way ANOVA and Tukey post hoc. ns, $P > 0.05$; *$P < 0.05$; ***$P < 0.001$.

agar, while the control group showed no preference (Fig. 8D and fig. S8D). The effects of Gr43a brain neurons in both the silencing and activation paradigms were dependent on starvation. Silencing Gr43a brain neurons produced no effect on preference for fructose over glucose in fed flies, although there was a reduction in overall feeding (fig. S8A). Similarly, activation in the STROBE also had no effect without starvation (fig. S8, D and E). This fits with the established model for Gr43a brain neuron function, where feeding promotion is only observed in starved flies (*24*).

DISCUSSION

Regulation of energy intake is a complex process involving food search, an animal's internal state, and the sensory qualities of food. In flies, fructose, either consumed directly or rapidly metabolized from precursors, promotes feeding through activation of a brain fructose sensor called Gr43a (*24*). Here, we describe how a neuronal network composed of neurons in the FB and asymmetric body contributes to energy homeostasis by detecting satiety-dependent changes in hemolymph glucose and modulating fructose drive (Fig. 8E).

The FB is a very organized yet incompletely understood structure

The central complex, which is composed of the FB, the protocerebral bridge (PB), the ellipsoid body, and the noduli, is regarded as a center for sensorimotor integration that functions in goal-directed behavior (*31*, *33*, *54*–*58*). The FB is organized in nine horizontal layers and nine vertical columns. FB large field neurons of layers 1 to 3,

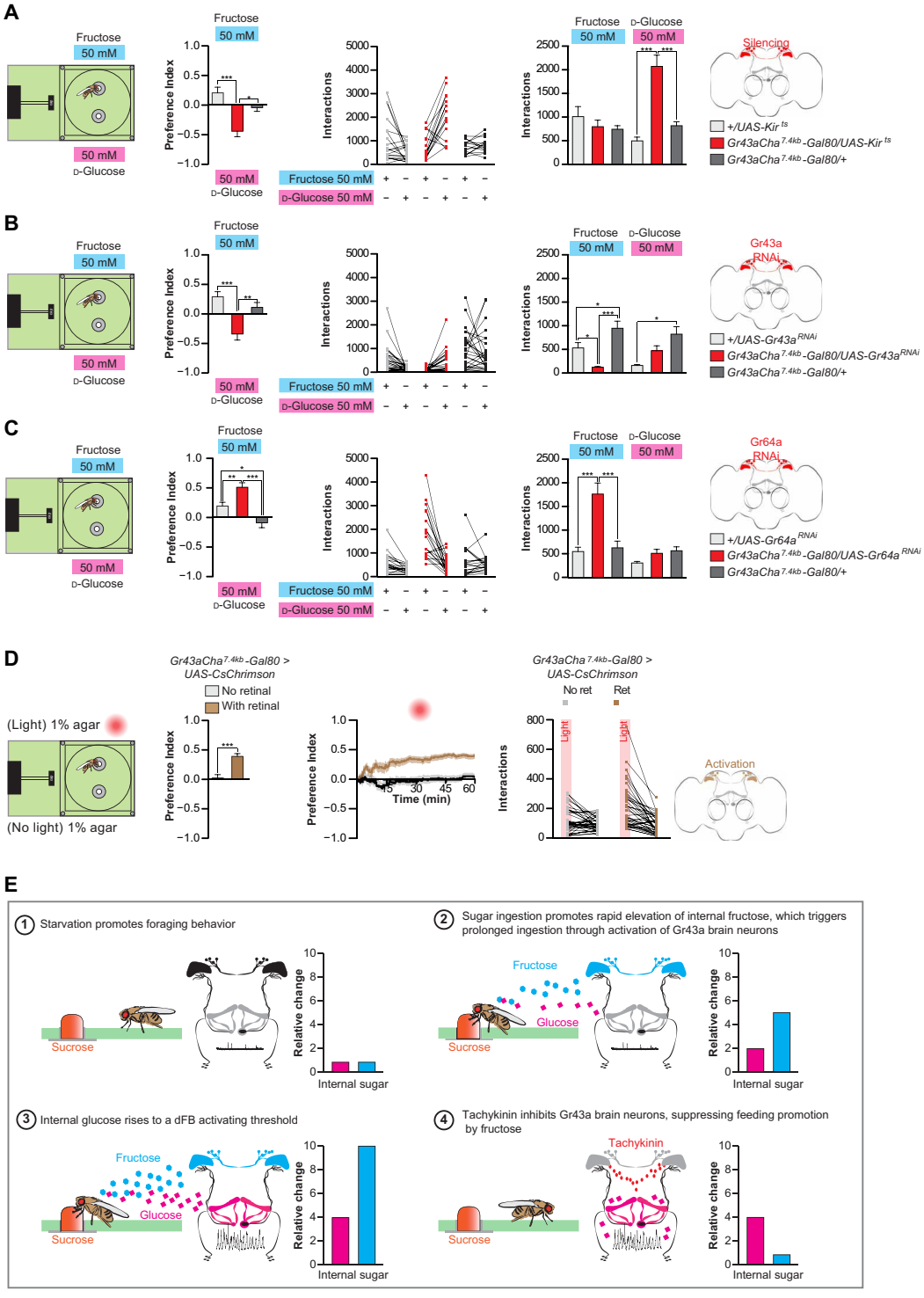

Fig. 8. Gr43a brain neurons acutely regulate feeding. (**A**) Effect of Gr43a brain neuron silencing on preference between fructose and D-glucose after 24-hour starvation and their corresponding interactions ($n = 15$ to 19). (**B**) Effect of Gr43a knockdown in Gr43a brain neurons on preference between fructose and D-glucose after 20-hour starvation and their corresponding interactions ($n = 22$ to 28). (**C**) Effect of Gr64a knockdown in Gr43a brain neurons on preference between fructose and D-glucose after 20-hour starvation and their corresponding interactions ($n = 19$ to 22). (**D**) Closed-loop activation of Gr43a brain neurons in the STROBE produces preference for the light-triggering food after 20-hour starvation, with corresponding interactions ($n = 40$ to 41). (**E**) Model for how fructose serves as a cue for promoting sugar ingestion and how rising glucose levels signal satiety through dFB neurons, which then inhibit sensitivity to fructose and terminate feeding. Values represent mean ± SEM. Statistical tests: one-way ANOVA, Tukey post hoc, and *t* test for CsChrimson experiment. ns, $P > 0.05$; *$P < 0.05$; ***$P < 0.001$.

and inputs to these layers from the PB, encode flight direction and general sensory orientation (*56*, *59*). FB layers 6 and 7 are well known to regulate sleep and arousal (*60*–*62*), locomotor control (*63*), courtship (*64*), visual memory (*65*–*67*), and decision-making related to taste (*68*). Layer 6 also plays a role in avoiding conditioned odors, while layers 1, 2, 4, and 5 respond to electric stimuli and are required for innate odor avoidance (*69*). However, the function of the most dorsal FB layers (8 and 9), mostly innervated local tangential neurons and AB-FBl8 (or vΔA_a), remained poorly understood (*28*, *31*–*33*). Our results demonstrate a role for these layers in feeding regulation.

dFB and Janus neurons provide insight into asymmetric body function

We find that dFB oscillations require glutamatergic input from Janus neuron projections to the asymmetric body. Described for the first time in 2004 (*38*), very little is known about AB function; 92.4% of flies display asymmetry in the AB, with the body present only in the right hemisphere, while 7.6% also have a body on the left side (*38*). We noted that oscillations in the dFB display a tendency to be faster on the right side, with clearly asynchronous activity between the two sides that may reflect their asymmetric input from Janus neurons. The small proportion of flies displaying symmetry in the AB have defects in LTM, a process that is known to require energy (*10*, *11*, *21*, *38*). We speculate that these symmetric flies may have a dysfunctional Janus neurons–to–dFB connection, resulting in impaired Tk release. This could affect LTM either directly or through changes in feeding. A role for TK in memory has been demonstrated in honeybees (*70*–*72*) and mammals (*73*), and TkR86C appears to be expressed in serotonergic paired neurons known to interact with MB-MP1 neurons required for LTM formation (*49*, *74*). Tk also acts through TkR99D to modulate activity in neurons producing insulin-like peptides (*47*, *75*), which affect LTM formation (*76*, *77*).

Modulation of dFB oscillations by Janus neurons requires glutamatergic signaling through a group of glutamate receptors including KaiR1D, NmdaR1, NmdaR2, and GluClα, but not AMPA receptors. Both KaiR1D receptors, which are homomeric (*40*), and *N*-methyl-D-aspartate (NMDA) receptors, which are heteromeric complexes between subunits 1 and 2, pass Ca^{2+} current (*42*). NMDA receptors (NMDAR) are well known for their role in mediating synaptic plasticity and can also trigger oscillatory activity (*42*, *78*). NMDAR function as molecular coincidence detectors, requiring simultaneous ligand binding and membrane depolarization for activation (*18*, *42*). It is possible that dFB neuron oscillations are triggered by the coincident detection of glutamate from Janus neurons and glucose from the hemolymph; however, because the FB are receiving many inputs from other brain region, we suspect that dFB oscillations require additional inputs as well. The chloride channel GluClα is also required for dFB oscillations. GluClα has been previously implicated in on/off responses of the visual system of flies and memory retention in honeybees, demonstrating a role in regulating cell excitability (*79*, *80*). Perhaps, GluClα functions in repolarization of the dFB neurons between calcium bursts. Further study will be required to fully understand how the suite of glutamate receptors function together to drive oscillations, along with the source of input to Janus neurons in the protocerebrum.

Separable roles for glucose and fructose

Because glucose is the primary circulating energy source, one might intuitively expect that enhancing feeding in response to postingestive glucose detection would be the most efficient means of optimizing energy uptake. However, using elevation of hemolymph glucose as a signal to continue feeding is problematic because glucose levels are tightly regulated and elevated glucose serves as a signal of satiety. On the other hand, internal fructose can vary widely in response to ingestion and can therefore be a more reliable indicator of recent sugar intake (*24*). Thus, the separation of glucose as a satiety indicator and fructose as marker of sugar consumption removes the potential ambiguity of each as a signal. Moreover, fructose typically coexists with other nutritive sugars in common food sources. Therefore, it may not be the case that flies specifically benefit from fructose intake but rather that fructose serves as an effective proxy for general carbohydrate ingestion. By using fructose and the narrowly tuned Gr43a fructose receptor to survey sugar consumption, flies can effectively benefit from both a fructose-mediated positive feedback loop and glucose-mediated negative feedback to co-operatively ensure appropriate energy intake.

Our finding that dFB glucose sensing modulates fructose feeding via Gr43a brain neurons fits with the established model of Gr43a brain neurons as central fructose sensors. For this mechanism to effectively sustain feeding on a rich sugar source, ingested sugars must rapidly increase fructose signaling to Gr43a brain neurons, which then must acutely promote feeding. While the precise kinetics of internal fructose elevation after sugar consumption have not been quantified, fructose levels in the head rapidly increase 10-fold after fructose feeding and then return to baseline (*24*). The role of direct fructose sensing by Gr43a brain neurons is highlighted by our observation that Gr43a knockdown in those neurons results in markedly lower relative intake of fructose compared to glucose (Fig. 8B). Unexpectedly, knockdown of Gr64a, another sugar receptor expressed in the same neurons, produced the opposite effect (Fig. 8C). This could be because Gr64a contributes to modulation of Gr43a brain neurons by other sugar cues, and the absence of this activity makes Gr43a-mediated fructose responses more pronounced. Alternatively, Gr43a may be expressed more strongly after Gr64a knockdown, leading to an increased fructose response.

Little is known about the mechanisms downstream of Gr43a brain neurons that promote feeding. All Gr43a brain neurons express the peptide Crz (*25*), but knockdown of Crz expression produced no significant effect on fructose preference over glucose. This suggests an important functional role for another neurotransmitter, although it is also possible that the RNAi knockdown was not effective. Irrespective of mechanism, two of our experiments support the idea that activation of Gr43a neurons acutely enhances feeding. First, silencing of dFB neurons by genetic manipulation or prolonged starvation produces Gr43a-dependent fructose preference within the first 10 min of a flyPAD assay (fig. S1C). Second, closed-loop optogenetic activation of Gr43a brain neurons was sufficient to produce a strong positive preference within 10 min in the STROBE (Fig. 8D).

The separable functions of glucose and fructose sensing in flies bear notable resemblance to the differential effects of these two sugars in the mammalian hypothalamus. In particular, AMPK expression in the arcuate nucleus of the hypothalamus is known to link energy levels to food drive. When glycemia is low, AMPK is activated and thereby promotes feeding through orexigenic AgRP/NPY neuron activity. Glucose administration suppresses activity in these peptidergic neurons, while fructose can have the opposite effect and promote further feeding (*81*–*83*). The first description of fly Gr43a neurons noted their orexinegenic activity and suggested a

potential functional homology with the hypothalamus (*24*). In the present study, we uncovered a multilayered neural system centered on a brain energy sensor (dFB), whose activation by glucose leads to anorexigenic behavior through inhibition of the brain fructose sensor Gr43a. Thus, our results are consistent with at least partial functional homology between the mammalian hypothalamus and brain Gr43a neurons of the fly.

MATERIALS AND METHODS

Drosophila melanogaster

Fly stocks were raised on standard food at 25°C and 70% relative humidity under a 12-hour light/12-hour dark cycle. For neuronal silencing experiments, we used *UAS-Kir2.1* alone or with *tub-Gal80*^{ts} (abbreviated *UAS-Kir*^{ts} in figures), and *LexAop-tnt*. For neuronal activation experiments, we used *UAS-dTrpA1* and *20XUAS-IVS-CsChrimson.mVenus* (Bloomington #55135). Specific FB expression was driven using *R70H05-GAL4* [(*28*); Bloomington #39554], *R70H05-LexA* [(*28*); Bloomington #54255], *VT005528-GAL4* [Vienna Drosophila Resource Center (VDRC)], and a newly built split-Gal4 line (*VT038216.P65; VT017124.DBD*). Specific SLP-AB expression was driven using *R72A10-GAL4* [(*28*); Bloomington #48306], *R72A10-LexA* [(*28*); Bloomington #54191], and a newly built split-GAL4 line (*R72A10.P65; R37G11.DBD*). Specific Gr43a expression was driven using *Gr43a*^{GAL4} (knock-in) and *Gr43aGal4,Cha*$^{7.4kb}$*-GAL80* [(*24*); gift from H. Amrein]. For staining experiments, we used *40XUAS-IVS-mCD8::GFP* (Bloomington #32195), *26XLexAop2-mCD8::GFP* (Bloomington #77124), *Trans-Tango* [(*39*); Bloomington #77124], *20XUAS-IVS-CsChrimson* (Bloomington #55136), and *UAS-DenMark,UAS-Syt* (Bloomington #33065). For GRASP experiment, we used *UAS-CD4::spGFP1-10* and *LexAop-CD4::spGFP11* (*37*). For imaging experiments, we used the *20XUAS-IVS-GCaMP6f* (Bloomington #42747). For RNAi experiments, we used RNAi against Glut1 (Bloomington #40904), HexC (Bloomington #57404), Vglut (Bloomington #40927), Vglut (Bloomington #27538), Vglut (Bloomington #40845) GluCla (Bloomington #53356), glutamate receptor IA (GluRIA) (Bloomington #40844), glutamate receptor IB (GluRIB) (Bloomington #40908), KaiR1D (Bloomington #25852), NmdaR1 (Bloomington #25941), NmdaR2 (Bloomington #40846), metabotropic Glutamate Receptor (mGluR) (Bloomington #34872), Gr43a (Bloomington #64881), Gr64a (VDRC #112930), sNPF (Bloomington #25867), Tk (Bloomington #25800), TkR 99D (Bloomington #27513), TkR86C (Bloomington #31884), and Crz (Bloomington #25999). The Crz, sNPF, and TkR86C RNAi lines, which produced no effects in our assays, have been previously verified for functionality (*47*, *84*, *85*).

Method details

Fly preparation and behavior experiments

All experiments were performed with mated female flies to reduce variability, given that sex differences were not a subject of investigation. After eclosion, flies were kept for 2 to 3 days in fresh vials containing standard medium. For thermosensitive silencing experiments (Kir^{ts}), flies were then transferred into vials for 2 days at 29°C. Flies were subjected to a varying fasting period (0 to 30 hours) where they were transferred to vials containing 1 ml of 1% agar at 29°C. For silencing (*UAS-kir2.1*; *LexAop-tnt*) and RNAi experiments, flies were transferred into vials containing 1 ml of 1% agar at 29°C for 15 to 18 hours. For activation experiments (dTrpA1), flies were transferred into vials containing 1 ml of 1% agar at 22°C for 43 to 45 hours. For STROBE experiments, flies were kept for several days in fresh vials containing standard medium and were then transferred at 25°C into vials covered with aluminum foil containing 1 ml of standard medium (control flies) or 1 ml of standard medium containing 1 mM all-*trans*-retinal (retinal flies) for 2 days. Flies were then subjected to a 24-hour fasting period where they were transferred to covered vials containing 1 ml of 1% agar (control flies) or 1 ml of 1% agar mixed with 1 mM all-*trans*-retinal (retinal flies). Sucrose, L-glucose, D-glucose, D-sorbitol, D-fructose, and agar were obtained from Sigma-Aldrich.

flyPAD experiments

All flies were 5 to 9 days old at the time of the assay, and experiments were performed between 10:00 a.m. and 5:00 p.m. For single-tastant experiments, one channel of the arena was loaded with 3.5 μl of 1% agar mixed with a tastant. To exclude interactions due to drinking behavior, the other side was loaded with 3.5 μl of 1% agar. The tastants used were sucrose (5, 50, and 1000 mM), L-glucose (5, 50, and 1000 mM), 50 mM L-glucose combined with D-sorbitol (0, 5, 50, 500, and 1000 mM), D-glucose (5, 50, and 1000 mM), fructose (5, 50, and 1000 mM), and D-sorbitol (50 mM). For dual-tastant experiments, one channel was loaded with fructose, while the other one was loaded with D-glucose, always in an equimolar manner (5, 50, and 1000 mM). Acquisition on the flyPAD software was started, and then single flies were transferred into each arena by mouth aspiration. Experiments were run for 60 min, and the preference index (PI) for each fly was calculated as: (interactions with food 1 – interactions with food 2)/(interactions with food 1 + interactions with from food 2). Tastants were all obtained from Sigma-Aldrich.

STROBE experiments

Experiments were performed as previously described (*35*). All flies were 5 to 9 days old at the time of the assay, and experiments were performed between 10:00 a.m. and 5:00 p.m. Both channels of the arena were loaded with 3.5 μl of 1% agar. Acquisition on the STROBE software was started, and then, single flies were transferred into each arena by mouth aspiration. Experiments were run for 60 min, and the PI for each fly was calculated as (interactions with food 1 – interactions with food 2)/(interactions with food 1 + interactions with from food 2). The red light-emitting diode is always associated to the left side (food 1), with a light intensity of 11.2 mW/cm^2. Agar and all-*trans*-retinal were obtained from Sigma-Aldrich (*35*).

Binary choice assay

Female flies aged 2 to 5 days were sorted into groups of 10 and were transferred starved as explained above. For the assays, flies were then transferred into testing vials containing six 10-μl dots of agar that alternated in color. The food choices were 1% agar with 50 mM fructose (food 1) and 1% agar with 50 mM D-glucose (food 2). Each choice contained either blue (0.125 mg/ml; Erioglaucine, FD and C Blue#1) or red (0.5 mg/ml; Amaranth, FD and C Red#2) dye, and half the replicates for each experiment were done with the dyes swapped to control for any dye preference. Flies were allowed to feed for 2 hours in the dark at 29°C and then frozen and scored for abdomen color. PI was calculated as [(# of flies labeled with food 1 color) – (# of flies labeled with food 2 color)]/(total number of flies that fed) (*35*).

Proboscis extension reflex

For tarsal PER, flies were mounted on glass slides using nail polish. For labellar PER, flies were placed inside a pipette tip cut to size so that only the head was exposed. Flies were then sealed into the tube with tape and then adhered to a glass slide with double-sided tape.

Flies were allowed 1 to 2 hours to recover before testing began. Flies were stimulated with water on their front tarsi or labella for tarsal and labellar PER, respectively, and allowed to drink until satiated. Each fly was then stimulated with increasing concentration of either D-glucose or fructose on either the tarsi or labella, and responses to each tastant were recorded. Flies were provided with water between each tastant. All stimuli were delivered with a 1-ml syringe attached to a 20-μl pipette tip (*86*).

In vivo calcium imaging

Female flies aged 5 to 9 days were briefly anesthetized. With a custom chamber, each fly was mounted by insertion of the cervix into individual collars. For further immobilization of the head, nail polish was applied in a thin layer to seal the head to the chamber. The antennae and the associated cuticle covering the subesophageal zone (SEZ) were removed until the ocelli, and adult hemolymph-like buffer with ribose was immediately injected into the preparation to cover the exposed brain. Flies were left to recover from anesthesia for an hour before imaging. At the beginning and end of the experiment, spontaneous or brush tickling–evoked leg or abdomen movement was checked to ensure that the fly was still alive (*10*, *11*).

GCaMP6f fluorescence was imaged with a Leica SP5 II laser scanning confocal microscope equipped with a tandem scanner and HyD detector. The relevant area of the FB was visualized using the 25× water objective. Images were acquired at a speed of 8000 lines/s with a line average of 1, resulting in a collection time of 0.051 ms per frame at a resolution of 256 × 126 pixels for a total of 7 min. The pinhole was opened to 200 μm (*86*).

Image analysis was performed following a previously described protocol (*10*, *11*). It was performed offline with a custom-written MATLAB program. Light intensity was averaged over a region of interest (ROI) delimited by hand and surrounding the projections of AB-FBl8 neurons on the FB layers 8 and 9. Three areas of interest (ROIs) were analyzed: the tips and the central part. From a given ROI, the resulting time trace was normalized to a percent change of fluorescence (100 $(F - F_0) / F_0$), using a baseline value of the fluorescence F_0 that was estimated as the mean fluorescence over the whole acquisition. To remove long-term drift, a baseline resulting from the moving average over a 100-s time window was then subtracted from the signal. Thus, in subsequent frequency analyses, all frequency axes are presented starting at 0.01 Hz. Given that signals are noisy, their amplitudes were estimated as the difference between the means of the 30% upper and lower quantiles of data points. For each signal, the power spectrum was computed and smoothed over a frequency window of 0.02 Hz. Rhythmic spontaneous activity in the time domain resulted in a peak in the power spectrum that had a finite width, as oscillations are intrinsically noisy. A fit of a Lorentzian curve to the power spectrum was performed to yield an estimate of the central frequency of the peak, f_0, and the width of the peak at half its maximal value, $\Delta f \cdot f_0$ defined the characteristic frequency of the oscillation, and frequency fluctuations around f_0, and hence the regularity of the oscillation, could be quantified by the quality factor $Q = f_0/\Delta f$ (*87*). A quality factor greater than 0.5 indicates that the zero frequency is excluded from the peak: This value was thus taken as a threshold to define a signal as rhythmically oscillating. When the fitting procedure converged to a value below 0.5, it was thus irrelevant to define oscillating parameters, and f_0 and Q were both assigned zero values.

To plot average amplitude histograms, we calculated a mean amplitude value for the different ROI selected, and then averaged the mean values across all flies from the same condition. Average power spectra across all animals from the same condition were obtained and were additionally smoothed over a 0.03-Hz frequency window. Peaked average spectra (Figs. 1D, 3E, 4G, and 5D and figs. S1, A, B, and I to K, and S3C) were characterized by their mean frequency f_0 and a quality factor Q calculated from f_0 and the width at half-height. For the refeeding experiment (Fig. 3D), flies were placed in vials containing agar 1% mixed with 500 mM D-glucose or 500 mM fructose for 30 min before the imaging experiment.

Immunohistochemistry

For GFP, brain immunofluorescence was carried out as described previously (*88*). Primary antibodies used were rabbit anti-GFP (1:1000, Invitrogen) and mouse anti-nc82 [1:50; Developmental Studies Hybridoma Bank (DSHB)]. Secondary antibodies used were goat anti-rabbit Alexa 488 (1:200; Invitrogen) and goat anti-mouse Alexa 568 (1:200; Invitrogen). For DenMark, Syt immunofluorescence, primary antibodies used were chicken anti-GFP (1:1000; Abcam) and rabbit anti-RFP (1:200; Rockland). Secondary antibodies used were goat anti-chicken Alexa 488 (1:200; Abcam) and goat anti-rabbit Alexa 647 (1:200; Thermo Fisher Scientific, Waltham, MA, #A21245). For GRASP immunofluorescence, primary antibodies used were mouse anti-GFP (1:100; Sigma-Aldrich, catalog no. G6539) and rabbit anti-DsRed (1:2000; Clontech, #632496). Secondary antibodies used were goat anti-mouse Alexa 488 (1:200; Invitrogen) and goat anti-rat Alexa 568 (1:200; Invitrogen). For *trans*-Tango immunofluorescence, primary antibodies were rabbit anti-GFP (1:1000; Invitrogen), mouse anti-nc82 (1:50; DSHB), and rat anti-hemagglutinin (1:100; Roche). Secondary antibodies used were goat anti-rabbit Alexa 488 (1:200; Invitrogen), goat anti-mouse Alexa 568 (1:200; Invitrogen), and goat anti-rat Alexa 647 (1:200; Invitrogen). For tachykinin immunofluorescence, flies dissected were either fed or starved for 30 hours at 29°C. Primary antibodies were chicken anti-GFP (1:1000; Abcam) and guinea pig anti-Tk (1:2000). Secondary antibodies used were goat anti-chicken Alexa 488 (1:200; Abcam) and goat anti–guinea pig Alexa 647 (1:200; Jackson ImmunoResearch) (*50*). All images were acquired using a Leica SP5 II confocal microscope with a 25× water immersion objective. All images were taken sequentially with a z-stack step size at 1 μm, a line average of 2, line-scanning speed of 200 Hz, and a resolution of 1024 × 1024 pixels. For tachykinin immunofluorescence, images were acquired using a Leica SP5 II confocal microscope with a 63× oil immersion objective. All images were taken sequentially with a z-stack step size at 0.5 μm, a line average of 2, line-scanning speed of 200 Hz, and a resolution of 1024 × 1024 pixels. Images were processed in ImageJ (*89*).

Quantification and statistical analysis

Statistical tests were performed using GraphPad Prism 6 software. Descriptions and results of each test are provided in the figure legends. Sample sizes are indicated in the figure legends. Sample sizes were determined before experimentation based on the variance and effect sizes seen in prior experiments of similar types. Whenever possible, all experimental conditions were run in parallel and therefore have the same or similar sample sizes.

All replicates were biological replicates using different flies. Data for all quantitative experiments were collected on at least three different days, and behavioral experiments were performed with flies from at least two independent crosses. Specific definitions of replicates are as follows. For calcium imaging, each data point represents the activity of a single fly to the indicated condition. For binary

choice behavioral tests, each data point represents the calculated preference for a group of 10 flies. For PER, each replicate is composed of 10 independent flies tested in parallel. For flyPAD and STROBE experiments, each data point is the calculated preference of an individual fly over the course of the experiment (*35*).

There were two conditions where data were excluded that were determined before experimentation and applied uniformly throughout. First, in calcium imaging experiments, all the data from a fly were removed if either (i) there was too much movement during the recording to reliably quantify the response or (ii) flies were dead at the end of the recording. Second, for flyPAD and STROBE experiments, the data from individual flies were removed if the fly did not pass a set minimum threshold of sips (*10*) or the data showed hallmarks of a technical malfunction (rare) (*35*).

For Tk immunostaining, fluorescence was quantified as follows: the cells of interest were selected, and their area, integrated density, and mean gray values were measured. The background values for these parameters were also recorded by selecting a region that has no fluorescence near the cells of interest. The corrected total cell fluorescence (CTCF) was then calculated using the equation: CTCF = integrated density − (area of selected cell × mean fluorescence of background readings). For each brain, 12 cells were randomly selected and quantified. Each replicate (n) corresponds to the CTCF of the 12 cells averaged for a brain (*90*). No ethics committee approval was needed for this study.

SUPPLEMENTARY MATERIALS

Supplementary material for this article is available at https://science.org/doi/10.1126/sciadv.abj0186

View/request a protocol for this paper from *Bio-protocol*.

REFERENCES AND NOTES

1. M. T. Le, R. F. Frye, C. J. Rivard, J. Cheng, K. K. McFann, M. S. Segal, R. J. Johnson, J. A. Johnson, Effects of high-fructose corn syrup and sucrose on the pharmacokinetics of fructose and acute metabolic and hemodynamic responses in healthy subjects. *Metabolism* **61**, 641–651 (2012).
2. M. A. Payant, M. J. Chee, Neural mechanisms underlying the role of fructose in overfeeding. *Neurosci. Biobehav. Rev.* **128**, 346–357 (2021).
3. B. Merino, C. M. Fernández-Díaz, I. Cózar-Castellano, G. Perdomo, Intestinal fructose and glucose metabolism in health and disease. *Nutrients* **12**, 94 (2019).
4. Y. Niwano, T. Adachi, J. Kashimura, T. Sakata, H. Sasaki, K. Sekine, S. Yamamoto, A. Yonekubo, S. Kimura, Is glycemic index of food a feasible predictor of appetite, hunger, and satiety? *J. Nutr. Sci. Vitaminol.* **55**, 201–207 (2009).
5. M. Dus, S. Min, A. C. Keene, G. Y. Lee, G. S. B. Suh, Taste-independent detection of the caloric content of sugar in *Drosophila*. *Proc. Natl. Acad. Sci. U.S.A.* **108**, 11644–11649 (2011).
6. G. Lee, J. H. Park, Hemolymph sugar homeostasis and starvation-induced hyperactivity affected by genetic manipulations of the adipokinetic hormone-encoding gene in *Drosophila melanogaster*. *Genetics* **167**, 311–323 (2004).
7. M. Dus, J. S. Y. Lai, K. M. Gunapala, S. Min, T. D. Tayler, A. C. Hergarden, E. Geraud, C. M. Joseph, G. S. B. Suh, Nutrient sensor in the brain directs the action of the brain-gut axis in *Drosophila*. *Neuron* **87**, 139–151 (2015).
8. N. Kapan, O. V. Lushchak, J. Luo, D. R. Nässel, Identified peptidergic neurons in the *Drosophila* brain regulate insulin-producing cells, stress responses and metabolism by coexpressed short neuropeptide F and corazonin. *Cell. Mol. Life Sci.* **69**, 4051–4066 (2012).
9. Y. Oh, J. S. Y. Lai, H. J. Mills, H. Erdjument-Bromage, B. Giammarinaro, K. Saadipour, J. G. Wang, F. Abu, T. A. Neubert, G. S. B. Suh, A glucose-sensing neuron pair regulates insulin and glucagon in *Drosophila*. *Nature* **574**, 559–564 (2019).
10. P.-Y. Musso, P. Tchenio, T. Preat, Delayed dopamine signaling of energy level builds appetitive long-term memory in *Drosophila*. *Cell Rep.* **10**, 1023–1031 (2015).
11. P.-Y. Plaçais, S. Trannoy, G. Isabel, Y. Aso, I. Siwanowicz, G. Belliart-Guérin, P. Vernier, S. Birman, H. Tanimoto, T. Preat, Slow oscillations in two pairs of dopaminergic neurons gate long-term memory formation in *Drosophila*. *Nat. Neurosci.* **15**, 592–599 (2012).
12. R. Eckhorn, R. Bauer, W. Jordan, M. Brosch, W. Kruse, M. Munk, H. J. Reitboeck, Coherent oscillations: A mechanism of feature linking in the visual cortex? Multiple electrode and correlation analyses in the cat. *Biol. Cybern.* **60**, 121–130 (1988).
13. M. Wehr, G. Laurent, Odour encoding by temporal sequences of firing in oscillating neural assemblies. *Nature* **384**, 162–166 (1996).
14. G. Pfurtscheller, F. H. Lopes da Silva, Event-related EEG/MEG synchronization and desynchronization: Basic principles. *Clin. Neurophysiol.* **110**, 1842–1857 (1999).
15. E. Nyhus, T. Curran, Functional role of gamma and theta oscillations in episodic memory. *Neurosci. Biobehav. Rev.* **34**, 1023–1035 (2010).
16. K. Benchenane, P. H. Tiesinga, F. P. Battaglia, Oscillations in the prefrontal cortex: A gateway to memory and attention. *Curr. Opin. Neurobiol.* **21**, 475–485 (2011).
17. L. Marshall, N. Cross, S. Binder, T. T. Dang-Vu, Brain rhythms during sleep and memory consolidation: Neurobiological insights. *Physiology* **35**, 4–15 (2020).
18. D. Raccuglia, S. Huang, A. Ender, M.-M. Heim, D. Laber, R. Suárez-Grimalt, A. Liotta, S. J. Sigrist, J. R. P. Geiger, D. Owald, Network-specific synchronization of electrical slow-wave oscillations regulates sleep drive in *Drosophila*. *Curr. Biol.* **29**, 3611–3621.e3 (2019).
19. A. Sclafani, Post-ingestive positive controls of ingestive behavior. *Appetite* **36**, 79–83 (2001).
20. I. E. de Araujo, A. J. Oliveira-Maia, T. D. Sotnikova, R. R. Gainetdinov, M. G. Caron, M. A. L. Nicolelis, S. A. Simon, Food reward in the absence of taste receptor signaling. *Neuron* **57**, 930–941 (2008).
21. C. J. Burke, S. Waddell, Remembering nutrient quality of sugar in *Drosophila*. *Curr. Biol.* **21**, 746–750 (2011).
22. J. W. Stafford, K. M. Lynd, A. Y. Jung, M. D. Gordon, Integration of taste and calorie sensing in *Drosophila*. *J. Neurosci.* **32**, 14767–14774 (2012).
23. P.-Y. Plaçais, É. de Tredern, L. Scheunemann, S. Trannoy, V. Goguel, K. A. Han, G. Isabel, T. Preat, Upregulated energy metabolism in the *Drosophila* mushroom body is the trigger for long-term memory. *Nat. Commun.* **8**, 15510 (2017).
24. T. Miyamoto, J. Slone, X. Song, H. Amrein, A fructose receptor functions as a nutrient sensor in the *Drosophila* brain. *Cell* **151**, 1113–1125 (2012).
25. T. Miyamoto, H. Amrein, Diverse roles for the *Drosophila* fructose sensor Gr43a. *Fly* **8**, 19–25 (2014).
26. S. Fujii, A. Yavuz, J. Slone, C. Jagge, X. Song, H. Amrein, *Drosophila* sugar receptors in sweet taste perception, olfaction, and internal nutrient sensing. *Curr. Biol.* **25**, 621–627 (2015).
27. T.-W. Chen, T. J. Wardill, Y. Sun, S. R. Pulver, S. L. Renninger, A. Baohan, E. R. Schreiter, R. A. Kerr, M. B. Orger, V. Jayaraman, L. L. Looger, K. Svoboda, D. S. Kim, Ultrasensitive fluorescent proteins for imaging neuronal activity. *Nature* **499**, 295–300 (2013).
28. A. Jenett, G. M. Rubin, T. T. B. Ngo, D. Shepherd, C. Murphy, H. Dionne, B. D. Pfeiffer, A. Cavallaro, D. Hall, J. Jeter, N. Iyer, D. Fetter, J. H. Hausenfluck, H. Peng, E. T. Trautman, R. R. Svirskas, E. W. Myers, Z. R. Iwinski, Y. Aso, G. M. DePasquale, A. Enos, P. Hulamm, S. C. B. Lam, H. H. Li, T. R. Laverty, F. Long, L. Qu, S. D. Murphy, K. Rokicki, T. Safford, K. Shaw, J. H. Simpson, A. Sowell, S. Tae, Y. Yu, C. T. Zugates, A GAL4-driver line resource for *Drosophila* neurobiology. *Cell Rep.* **2**, 991–1001 (2012).
29. S. A. Escher, A. Rasmuson-Lestander, The *Drosophila* glucose transporter gene: cDNA sequence, phylogenetic comparisons, analysis of functional sites and secondary structures. *Hereditas* **130**, 95–103 (1999).
30. D. Moser, L. Johnson, C. Y. Lee, Multiple forms of *Drosophila* hexokinase. Purification, biochemical and immunological characterization. *J. Biol. Chem.* **255**, 4673–4679 (1980).
31. T. Wolff, N. A. Iyer, G. M. Rubin, Neuroarchitecture and neuroanatomy of the *Drosophila* central complex: A GAL4-based dissection of protocerebral bridge neurons and circuits. *J. Comp. Neurol.* **523**, 997–1037 (2015).
32. T. Wolff, G. M. Rubin, Neuroarchitecture of the *Drosophila* central complex: A catalog of nodulus and asymmetrical body neurons and a revision of the protocerebral bridge catalog. *J. Comp. Neurol.* **526**, 2585–2611 (2018).
33. B. K. Hulse, H. Haberkern, R. Franconville, D. B. Turner-Evans, S. Takemura, T. Wolff, M. Noorman, M. Dreher, C. Dan, R. Parekh, A. M. Hermundstad, G. M. Rubin, V. Jayaraman, A connectome of the *Drosophila* central complex reveals network motifs suitable for flexible navigation and context-dependent action selection. *bioRxiv* 10.1101/2020.12.08.413955 , (2020).
34. P. M. Itskov, J. M. Moreira, E. Vinnik, G. Lopes, S. Safarik, M. H. Dickinson, C. Ribeiro, Automated monitoring and quantitative analysis of feeding behaviour in *Drosophila*. *Nat. Commun.* **5**, 4560 (2014).
35. P.-Y. Musso, P. Junca, M. Jelen, D. Feldman-Kiss, H. Zhang, R. C. W. Chan, M. D. Gordon, Closed-loop optogenetic activation of peripheral or central neurons modulates feeding in freely moving *Drosophila*. *eLife* **8**, e45636 (2019).
36. Z. Wang, A. Singhvi, P. Kong, K. Scott, Taste representations in the *Drosophila* brain. *Cell* **117**, 981–991 (2004).
37. M. D. Gordon, K. Scott, Motor control in a *Drosophila* taste circuit. *Neuron* **61**, 373–384 (2009).
38. A. Pascual, K.-L. Huang, J. Neveu, T. Preat, Neuroanatomy: Brain asymmetry and long-term memory. *Nature* **427**, 605–606 (2004).
39. M. Talay, E. B. Richman, N. J. Snell, G. G. Hartmann, J. D. Fisher, A. Sorkaç, J. F. Santoyo, C. Chou-Freed, N. Nair, M. Johnson, J. R. Szymanski, G. Barnea, Transsynaptic mapping of second-order taste neurons in flies by trans-tango. *Neuron* **96**, 783–795.e4 (2017).

40. Y. Li, P. Dharkar, T. H. Han, M. Serpe, C. H. Lee, M. L. Mayer, Novel functional properties of *Drosophila* CNS glutamate receptors. *Neuron* **92**, 1036–1048 (2016).
41. L. Kahsai, M. A. Carlsson, A. M. E. Winther, D. R. Nässel, Distribution of metabotropic receptors of serotonin, dopamine, GABA, glutamate, and short neuropeptide F in the central complex of *Drosophila*. *Neuroscience* **208**, 11–26 (2012).
42. S. Xia, A.-S. Chiang, NMDA receptors in *Drosophila*, in *Biology of the NMDA Receptor*, A. M. Van Dongen, Ed. (CRC Press/Taylor & Francis, 2009).
43. M. O. Thorner, R. W. Holl, D. A. Leong, The somatotrope: An endocrine cell with functional calcium transients. *J. Exp. Biol.* **139**, 169–179 (1988).
44. J. Clements, T. Dolafi, L. Umayam, N. L. Neubarth, S. Berg, L. K. Scheffer, S. M. Plaza, neuPrint: Analysis tools for EM connectomics. *bioRxiv* 10.1101/2020.01.16.909465 , (2020).
45. A. M. E. Winther, R. J. Siviter, R. E. Isaac, R. Predel, D. R. Nässel, Neuronal expression of tachykinin-related peptides and gene transcript during postembryonic development of *Drosophila*. *J. Comp. Neurol.* **464**, 180–196 (2003).
46. L. Kahsai, A. M. E. Winther, Chemical neuroanatomy of the *Drosophila* central complex: Distribution of multiple neuropeptides in relation to neurotransmitters. *J. Comp. Neurol.* **519**, 290–315 (2011).
47. W. Qi, G. Wang, L. Wang, A novel satiety sensor detects circulating glucose and suppresses food consumption via insulin-producing cells in *Drosophila*. *Cell Res.* **31**, 580–588 (2021).
48. X. J. Li, W. Wolfgang, Y. N. Wu, R. A. North, M. Forte, Cloning, heterologous expression and developmental regulation of a *Drosophila* receptor for tachykinin-like peptides. *EMBO J.* **10**, 3221–3229 (1991).
49. J. Poels, R. T. Birse, R. J. Nachman, J. Fichna, A. Janecka, J. vanden Broeck, D. R. Nässel, Characterization and distribution of NKD, a receptor for *Drosophila* tachykinin-related peptide 6. *Peptides* **30**, 545–556 (2009).
50. K. Asahina, K. Watanabe, B. J. Duistermars, E. Hoopfer, C. R. González, E. A. Eyjólfsdóttir, P. Perona, D. J. Anderson, Tachykinin-expressing neurons control male-specific aggressive arousal in *Drosophila*. *Cell* **156**, 221–235 (2014).
51. R. T. Birse, E. C. Johnson, P. H. Taghert, D. R. Nässel, Widely distributed *Drosophila* G-protein-coupled receptor (CG7887) is activated by endogenous tachykinin-related peptides. *J. Neurobiol.* **66**, 33–46 (2006).
52. R. Ignell, C. M. Root, R. T. Birse, J. W. Wang, D. R. Nassel, A. M. E. Winther, Presynaptic peptidergic modulation of olfactory receptor neurons in *Drosophila*. *Proc. Natl. Acad. Sci. U.S.A.* **106**, 13070–13075 (2009).
53. N. C. Klapoetke, Y. Murata, S. S. Kim, S. R. Pulver, A. Birdsey-Benson, Y. K. Cho, T. K. Morimoto, A. S. Chuong, E. J. Carpenter, Z. Tian, J. Wang, Y. Xie, Z. Yan, Y. Zhang, B. Y. Chow, B. Surek, M. Melkonian, V. Jayaraman, M. Constantine-Paton, G. K. S. Wong, E. S. Boyden, Independent optical excitation of distinct neural populations. *Nat. Methods* **11**, 338–346 (2014).
54. Y. E. Fisher, J. Lu, I. D'Alessandro, R. I. Wilson, Sensorimotor experience remaps visual input to a heading-direction network. *Nature* **576**, 121–125 (2019).
55. K. Pfeiffer, U. Homberg, Organization and functional roles of the central complex in the insect brain. *Annu. Rev. Entomol.* **59**, 165–184 (2014).
56. P. T. Weir, M. H. Dickinson, Functional divisions for visual processing in the central brain of flying *Drosophila*. *Proc. Natl. Acad. Sci. U.S.A.* **112**, E5523–E5532 (2015).
57. A. Honkanen, A. Adden, J. da Silva Freitas, S. Heinze, The insect central complex and the neural basis of navigational strategies. *J. Exp. Biol.* **222**, jeb188854 (2019).
58. X. Sun, S. Yue, M. Mangan, A decentralised neural model explaining optimal integration of navigational strategies in insects. *eLife* **9**, e54026 (2020).
59. T. A. Currier, A. M. Matheson, K. I. Nagel, Encoding and control of orientation to airflow by a set of *Drosophila* fan-shaped body neurons. *eLife* **9**, e61510 (2020).
60. J. A. Berry, I. Cervantes-Sandoval, M. Chakraborty, R. L. Davis, Sleep facilitates memory by blocking dopamine neuron-mediated forgetting. *Cell* **161**, 1656–1667 (2015).
61. J. M. Donlea, M. S. Thimgan, Y. Suzuki, L. Gottschalk, P. J. Shaw, Inducing sleep by remote control facilitates memory consolidation in *Drosophila*. *Science* **332**, 1571–1576 (2011).
62. T. Ueno, J. Tomita, H. Tanimoto, K. Endo, K. Ito, S. Kume, K. Kume, Identification of a dopamine pathway that regulates sleep and arousal in *Drosophila*. *Nat. Neurosci.* **15**, 1516–1523 (2012).
63. R. Strauss, The central complex and the genetic dissection of locomotor behaviour. *Curr. Opin. Neurobiol.* **12**, 633–638 (2002).
64. T. Sakai, T. Kitamoto, Differential roles of two major brain structures, mushroom bodies and central complex, for *Drosophila* male courtship behavior. *J. Neurobiol.* **66**, 821–834 (2006).
65. W. Li, Y. Pan, Z. Wang, H. Gong, Z. Gong, L. Liu, Morphological characterization of single fan-shaped body neurons in *Drosophila* melanogaster. *Cell Tissue Res.* **336**, 509–519 (2009).
66. G. Liu, H. Seiler, A. Wen, T. Zars, K. Ito, R. Wolf, M. Heisenberg, L. Liu, Distinct memory traces for two visual features in the *Drosophila* brain. *Nature* **439**, 551–556 (2006).
67. Z. Wang, Y. Pan, W. Li, H. Jiang, L. Chatzimanolis, J. Chang, Z. Gong, L. Liu, Visual pattern memory requires foraging function in the central complex of *Drosophila*. *Learn. Mem.* **15**, 133–142 (2008).
68. P. F. Sareen, L. Y. McCurdy, M. N. Nitabach, A neuronal ensemble encoding adaptive choice during sensory conflict in *Drosophila*. *Nat. Commun.* **12**, 4131 (2021).
69. W. Hu, Y. Peng, J. Sun, F. Zhang, X. Zhang, L. Wang, Q. Li, Y. Zhong, Fan-shaped body neurons in the *Drosophila* brain regulate both innate and conditioned nociceptive avoidance. *Cell Rep.* **24**, 1573–1584 (2018).
70. H. Takeuchi, A. Yasuda, Y. Yasuda-Kamatani, M. Sawata, Y. Matsuo, A. Kato, A. Tsujimoto, T. Nakajima, T. Kubo, Prepro-tachykinin gene expression in the brain of the honeybee *Apis mellifera*. *Cell Tissue Res.* **316**, 281–293 (2004).
71. A. Brockmann, S. P. Annangudi, T. A. Richmond, S. A. Ament, F. Xie, B. R. Southey, S. R. Rodriguez-Zas, G. E. Robinson, J. V. Sweedler, Quantitative peptidomics reveal brain peptide signatures of behavior. *Proc. Natl. Acad. Sci. U.S.A.* **106**, 2383–2388 (2009).
72. B. Boerjan, D. Cardoen, A. Bogaerts, B. Landuyt, L. Schoofs, P. Verleyen, Mass spectrometric profiling of (neuro)-peptides in the worker honeybee, *Apis mellifera*. *Neuropharmacology* **58**, 248–258 (2010).
73. L. Lénárd, K. László, E. Kertes, T. Ollmann, L. Péczely, A. Kovács, V. Kállai, O. Zagorácz, R. Gálosi, Z. Karádi, Substance P and neurotensin in the limbic system: Their roles in reinforcement and memory consolidation. *Neurosci. Biobehav. Rev.* **85**, 1–20 (2018).
74. L. Scheunemann, P.-Y. Plaçais, Y. Dromard, M. Schwärzel, T. Preat, Dunce phosphodiesterase acts as a checkpoint for *Drosophila* long-term memory in a pair of serotonergic neurons. *Neuron* **98**, 350–365.e5 (2018).
75. R. T. Birse, J. A. E. Söderberg, J. Luo, A. M. E. Winther, D. R. Nässel, Regulation of insulin-producing cells in the adult *Drosophila* brain via the tachykinin peptide receptor DTKR. *J. Exp. Biol.* **214**, 4201–4208 (2011).
76. D. B. Chambers, A. Androschuk, C. Rosenfelt, S. Langer, M. Harding, F. V. Bolduc, Insulin signaling is acutely required for long-term memory in *Drosophila*. *Front Neural Circuits* **9**, 8 (2015).
77. M. Eschment, H. R. Franz, N. Güllü, L. G. Hölscher, K. E. Huh, A. Widmann, Insulin signaling represents a gating mechanism between different memory phases in *Drosophila* larvae. *PLOS Genet.* **16**, e1009064 (2020).
78. J. N. MacLean, B. J. Schmidt, S. Hochman, NMDA receptor activation triggers voltage oscillations, plateau potentials and bursting in neonatal rat lumbar motoneurons in vitro. *Eur. J. Neurosci.* **9**, 2702–2711 (1997).
79. S. Molina-Obando, J. F. Vargas-Fique, M. Henning, B. Gur, T. M. Schladt, J. Akhtar, T. K. Berger, M. Silies, ON selectivity in the *Drosophila* visual system is a multisynaptic process involving both glutamatergic and GABAergic inhibition. *eLife* **8**, e49373 (2019).
80. A. K. El Hassani, M. Giurfa, M. Gauthier, C. Armengaud, Inhibitory neurotransmission and olfactory memory in honeybees. *Neurobiol. Learn. Mem.* **90**, 589–595 (2008).
81. Y. Minokoshi, T. Alquier, N. Furukawa, Y. B. Kim, A. Lee, B. Xue, J. Mu, F. Foufelle, P. Ferré, M. J. Birnbaum, B. J. Stuck, B. B. Kahn, AMP-kinase regulates food intake by responding to hormonal and nutrient signals in the hypothalamus. *Nature* **428**, 569–574 (2004).
82. S. H. Cha, M. Wolfgang, Y. Tokutake, S. Chohnan, M. D. Lane, Differential effects of central fructose and glucose on hypothalamic malonyl-CoA and food intake. *Proc. Natl. Acad. Sci. U.S.A.* **105**, 16871–16875 (2008).
83. M. A. Burmeister, J. Ayala, D. J. Drucker, J. E. Ayala, Central glucagon-like peptide 1 receptor-induced anorexia requires glucose metabolism-mediated suppression of AMPK and is impaired by central fructose. *Am. J. Physiol. Endocrinol. Metab.* **304**, E677–E685 (2013).
84. Megha, C. Wegener, G. Hasan, ER-Ca^{2+} sensor STIM regulates neuropeptides required for development under nutrient restriction in *Drosophila*. *PLOS ONE*. **14**, e0219719 (2019).
85. Y. Shang, N. C. Donelson, C. G. Vecsey, F. Guo, M. Rosbash, L. C. Griffith, Short neuropeptide F is a sleep-promoting inhibitory modulator. *Neuron* **80**, 171–183 (2013).
86. E. E. LeDue, Y.-C. Chen, A. Y. Jung, A. Dahanukar, M. D. Gordon, Pharyngeal sense organs drive robust sugar consumption in *Drosophila*. *Nat. Commun.* **6**, 6667 (2015).
87. P.-Y. Plaçais, M. Balland, T. Guérin, J.-F. Joanny, P. Martin, Spontaneous oscillations of a minimal actomyosin system under elastic loading. *Phys. Rev. Lett.* **103**, 158102 (2009).
88. B. Chu, V. Chui, K. Mann, M. D. Gordon, Presynaptic gain control drives sweet and bitter taste integration in *Drosophila*. *Curr. Biol.* **24**, 1978–1984 (2014).
89. J. Schindelin, I. Arganda-Carreras, E. Frise, V. Kaynig, M. Longair, T. Pietzsch, S. Preibisch, C. Rueden, S. Saalfeld, B. Schmid, J. Y. Tinevez, D. J. White, V. Hartenstein, K. Eliceiri, P. Tomancak, A. Cardona, Fiji: An open-source platform for biological-image analysis. *Nat. Methods* **9**, 676–682 (2012).
90. M. Zandawala, T. Nguyen, M. Balanyà Segura, H. A. D. Johard, M. Amcoff, C. Wegener, J. P. Paluzzi, D. R. Nässel, A neuroendocrine pathway modulating osmotic stress in *Drosophila*. *PLOS Genet.* **17**, e1009425 (2021).

Acknowledgments: We thank members of the laboratory for comments on the manuscript. We thank P.-Y. Plaçais for providing the MATLAB code for oscillation analysis and for help in processing. We also thank H. Amrein, M. Wu, the Bloomington Stock Center, and the Vienna

Drosophila Resource Center for fly stocks. We also thank D. J. Anderson for providing the guinea pig antibody against tachykinin. **Funding:** This work was supported by the Natural Sciences and Engineering Research Council (NSERC) (RGPIN-2016-03857 and RGPAS-49246-16) (to M.D.G.) and a Michael Smith Foundation for Health Research Scholar Award (to M.D.G.).
Author contributions: Conceptualization, P.-Y.M. Methodology, P.-Y.M. and M.D.G. Formal analysis, P.-Y.M., P.J., and M.D.G. Investigation, P.-Y.M. and P.J. Writing, P.-Y.M. and M.D.G. Visualization, P.-Y.M. Supervision, M.D.G. Funding acquisition, M.D.G. **Competing interests:** The authors declare that they have no competing interests. **Data and materials availability:** All data needed to evaluate the conclusions in the paper are present in the paper and/or the Supplementary Materials. Raw numerical data are available for download from Zenodo at https://dx.doi.org/10.5281/zenodo.5534939.

Submitted 15 April 2021
Accepted 14 October 2021
Published 1 December 2021
10.1126/sciadv.abj0186